Soft Computing
https://doi.org/10.1007/s00500-023-09315-1

APPLICATION OF SOFT COMPUTING

Optimal solution for hydro–thermal–wind–solar scheduling using opposition-based whale optimization algorithm

Chandan Paul[1] · Provas Kumar Roy[2] · V. Mukherjee[3]

Accepted: 25 September 2023

Abstract

In the current research scenario, sincere effort has been taken worldwide to explore the use of renewable energy sources in electrical power system for the economic benefits and environmental consciousness. In this work, a relatively published new population-based optimization technique, called opposition-based whale optimization algorithm (WOA) (OWOA) having the ability to enhance the local search and speeding up the convergence speed of the solution, has been implemented to analyse the wind- and solar-based hydro–thermal scheduling with transmission losses. The main purpose of this work is to minimize the generation cost as well as emission by optimally scheduling the generation on hourly basis. This newly developed algorithm is initially tested on benchmark functions (high-dimensional complex problems) to establish the optimization capability of the algorithm as compared to the basic WOA counterpart. This optimization technique has the ability to handle the nonlinearity due to the presence of valve point loading in thermal power plant and the uncertainty of wind and solar for wind and solar-based power plant in practical situation. The proposed OWOA and the basic WOA are tested on hydro–thermal scheduling (HTS) and, finally, on HTS with wind and solar. The obtained results show that the generation cost and emission decrease with the incorporation of wind and solar in HTS system. Furthermore, the obtained results from OWOA for cost as well as emission minimization are compared with the WOA, grey wolf optimization (GWO), differential evolution (DE), quantum-inspired evolutionary algorithm (QEA), small population-based particle swarm optimization (SPSO), fuzzy-based evolutionary programming (Fuzzy EP), sine cosine algorithm (SCA) and backtracking search algorithm (BSA) for various cases to verify robustness of the proposed algorithm.

Keywords Hydro–thermal scheduling (HTS) · Hydro–thermal–wind–solar scheduling (HTWSS) · Opposition-based whale optimization algorithm (OWOA) · Solar energy · Wind energy

1 Introduction

At present, the demand for electricity goes on increasing, whereas the availability of conventional source of energy such as coal, petroleum and natural gas goes on decreasing. Furthermore, generation of electricity using fuels causes greenhouse effect. The rising environmental awareness desires short-term hydro–thermal scheduling (HTS) with renewable sources. Presently, the generation of electricity by renewable power plants is 33.6% of the total installed power generating capacity in India. The main objective of power generation using renewable sources is to reduce the generation cost as well as CO_2 emission while fulfilling various constraints of the generating units. Nowadays, the generation of power using wind and solar is being emphasized in view of clean, green energy source for more generation of power. The wind power plants have some difficulties such as uncertainties of wind which may cause an imbalance of wind power generation. This uncertainty of wind power may be reduced while using Weibull probability distribution function (PDF). The sun provides the most abundant, reliable and pollution-free power in the world. But solar panel does not produce electricity for 24 h a day. Point estimate method (PEM) helps to control the uncertainties

✉ Chandan Paul
chandan815@rediffmail.com

[1] Present Address: Department of Electrical Engineering, Dr. B. C Roy Engineering College, Durgapur, West Bengal 713206, India

[2] Department of Electrical Engineering, Kalyani Government Engineering College, Kalyani, West Bengal, India

[3] Department of Electrical Engineering, Indian Institute of Technology (Indian School of Mines), Dhanbad, Jharkhand, India

of solar radiation for solar power generation to meet power demand. Incorporation of wind and solar with HTS makes the problem more complex and nonlinear.

In view of the importance of HTS, many researchers are using various mathematical models to solve the problem. They have tried to employ classical optimization techniques like Lagrange relaxation (LR) (Salam et al. 1998), network flow (Qing et al. 1988), linear programming (Borghetti et al. 2008), dynamic programming (Jin-Shyr and Nanming 1989), quadratic programming (Petcharaks and Ongsakul 2007), and so on for obtaining satisfactory result of HTS problem. For the inherent complexity and nonlinearity of the scheduling problems, classical techniques are incapable of providing the global optimal solution. So, several evolutionary techniques are used to analyse the HTS problems.

Acharya et al. (2021) proposed multi-objective multiverse optimization algorithm for economic operation of generation cost and emission minimization with valve point loading effect for dynamic load dispatch problem. Parouha (2019) applied variant of the traditional particle swarm optimization (PSO) like modified time varying (PSO) (MTVPSO) to enhance the global searching ability for non-convex and nonsmooth economic load dispatch (ELD) problem. Parouha and Verma (2021) utilized innovative hybrid algorithm to avoid premature convergence and made a balance between the global and the local search capability for solving nonconvex ELD problem with and without valve point loading. Roy (2013) introduced a new approach, named as teaching learning-based optimization, to solve HTS problem where optimal solution of fuel cost is obtained through teaching learning process. Comparison of this algorithm with other optimization techniques established its effectiveness in the referred work. In the recent past, Bhattacharjee et al. (2014) introduced real-coded chemical reaction-based optimization to analyse the problem of HTS. This method works on the basis of the chemical reaction within the molecules to reach their stable position. This algorithm needs less number of iterations due to its good searching quality to obtain the solution. Cuckoo search algorithm (adopted by Nguyen et al. (2014)) requires less number of control parameters, and it helps to yield an excellent balance of randomization. Gouthamkumar et al. (2015) reported a disruptive-based gravitational search algorithm (GSA) to solve the HTS problem without considering transmission losses. Disruptive parameter helps to enhance the searching behaviour and exploitation capability of the algorithm. Improved searching behaviour of the algorithm increases the convergence speed.

Šulek et al. (2014) presented particle swarm optimization (PSO) method to analyse the HTS problem, which have some advantages over the other methods such as execution time and durability for controlling the parameters. Afterwards, improved PSO (IPSO), a new technique, was proposed by Hota et al. (2009) on HTS system. Different constraints were taken into consideration during solution of the problem such as prohibited operating zone, valve point loading and multireservoir. The authors Hota et al. (2009) proved that the convergence behaviour using IPSO is much faster than PSO technique. Zou et al. (2019) performed an experiment on combined heat and power to utilize the wasted heat from flue gases. The use of wasted heat helps to reduce the fuel cost as well as emission during power generation. Improved predator influenced civilized swarm optimization (Narang 2017) has been deployed to analyse the HTS problem. In this method, predator improved the exploration which will enhance the exploitation ability of the applied technique. Roy et al. (2018) utilized krill herd algorithm (KHA) where the local and the global search are controlled very effectively by using crossover and mutation operation. Cavazzini et al. (2018) introduced two swarm-based PSO search strategies to obtain optimal solution for the HTS problem. The first swarm assists to obtain feasible solution, and the next one deals with fewer solutions for repair approach.

Nazari-Heris et al. (2017) proposed real-coded genetic algorithm (GA) using improved Mühlenbein mutation for short-term HTS problem where optimal solutions have been obtained after considering hydro–thermal losses of the system. Non-dominated sorting genetic algorithm II (NSGA-II)-based multi-objective optimization was suggested by Dey et al. (2022) to solve economic environment dispatch problem of renewable energy sources in a way that is more authentic and effective. The EED problem, which involves competing and in-commensurable cost and emission objectives, was solved using multi-objective particle swarm optimization (MOPSO) technique (Abido 2009). The results demonstrated that the proposed MOPSO technique had the potential to solve the multi-objective problem. For the purpose of resolving the economic emission dispatch problem with valve point effect, Sundaram (2017) introduced the hybrid NSGA-II-based MOPSO, which successfully balanced the tasks of exploitation and exploration. However, the NSGA-II-based MOPSO (Dhiman 2020) strategy, which addresses economic and micro-grid power dispatch issues, suffers from low computational efforts. Multi-verse optimization algorithm (MOMVO), developed by Mirjalili et al. (2017), was used to tackle optimize problems having multiple objectives. MOMVO can solve both constrained and unconstrained multi-objective problems. However, while dealing with various problems, MVO (Aljarah et al. 2021) has local optima stagnation and is unable to sustain an optimal solution. Sundaram (2020) implemented MOMVO approach to solve the combined economic emission dispatch problems with considering different constraints. Additionally, Sundaram (2022) applied the same strategy to analyse a dynamic economic emission dispatch problem in which the trained neural network could only estimate the transmission loss

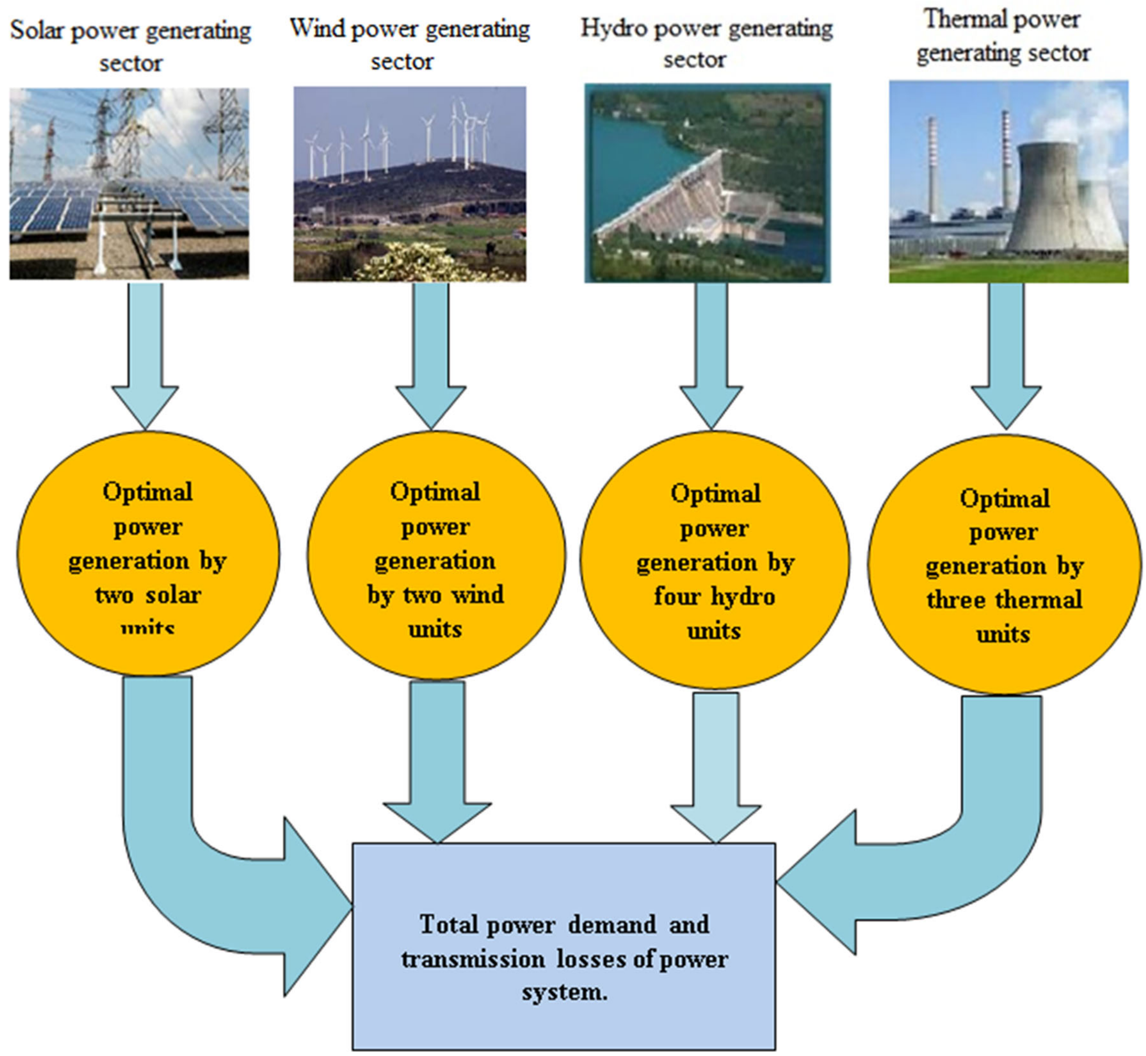

Fig. 1 Pictorial model of hydro–thermal–wind–solar optimal scheduling

once for each interval of the dispatch period. This results in a saving of fuel cost and a reduction of emission levels.

Furthermore, many researchers investigated the effect of non-conventional energy resources on HTS to reduce the generation price and emission. But the power system stability function may be affected by the uncertainty of wind and solar power during electrical power generation. Various optimization techniques, as employed by many researchers to deal with nonlinearity due to wind and solar uncertainty, are discussed below.

Hazra and Roy (2020) implemented moth-flame optimization (MFO) technique on renewable energy-based HTS problem. In this scheduling, HTS was integrated with wind energy sources to minimize both generation cost and emission. Again, Hazra and Roy (2021) tested the MFO technique on more nonlinearity-based HTS system incorporated with wind and solar energy sources to obtain the optimal solution for economic power generation and emission minimization. Dasgupta et al. (2020) proposed sine cosine algorithm on HTS system, where wind energy source had been scheduled to obtain the optimal solution over power generation and emission. The uncertainties due to randomness of air were resolved using Weibull probability density function. Patwal and Narang (2020) proposed scheduling of wind energy source with HTS and pumped storage and analysed in terms of cost. A modified crisscross PSO (MCPSO) was tested on three different test systems to deal with continuous decision variables for optimal solution.

Panda et al. (2017) implemented modified bacteria foraging algorithm on HTS-wind problem with static compensator which provides less generation cost, and bus voltages remain constant with variation of load. Basu (2019) proposed NSGA-II to solve dynamic economic emission dispatch problem where both cost and emission are minimized simultaneously. For economic emission dispatching in HTS-wind problem, modified GSA has been applied by Chen et al.

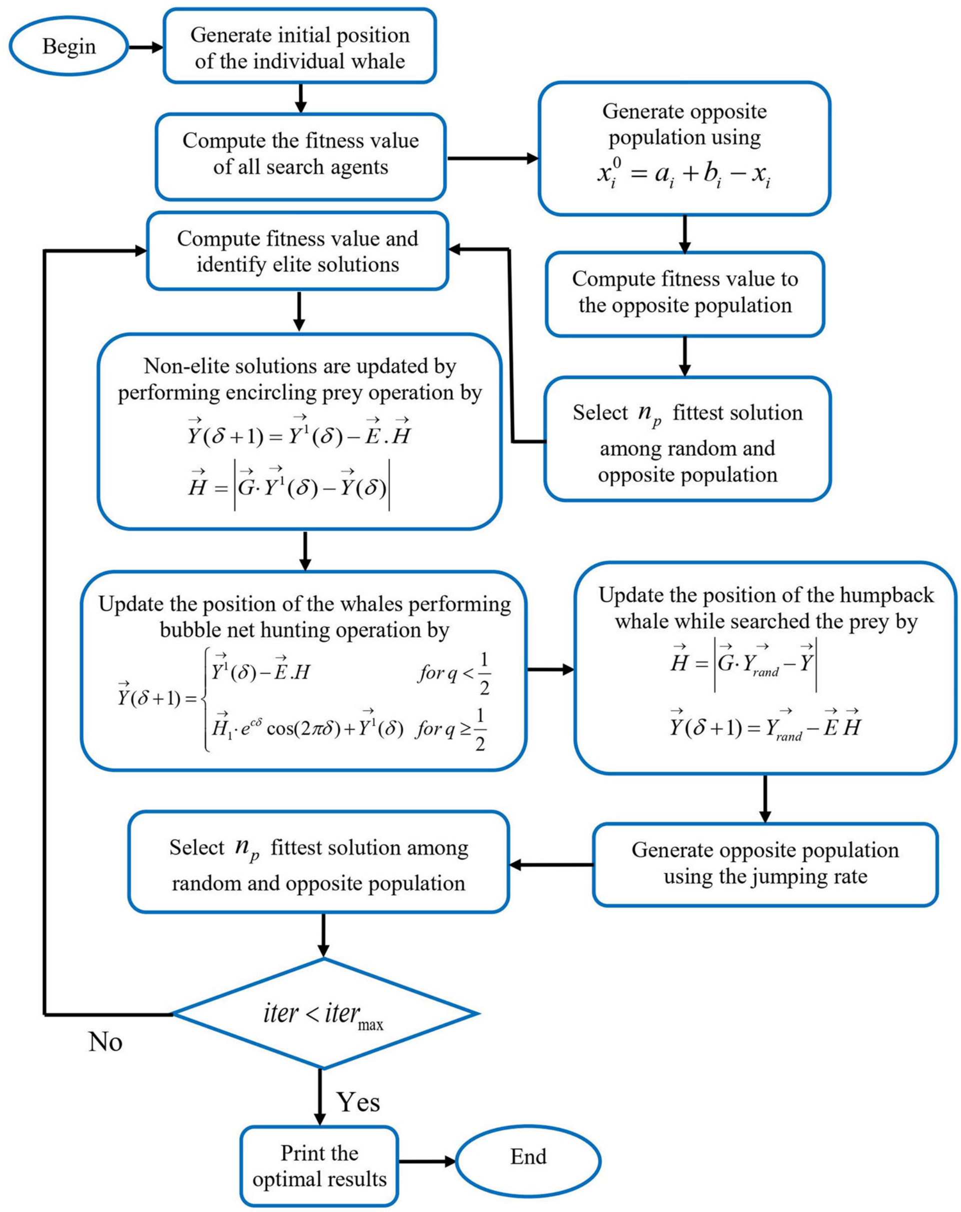

Fig. 2 Flow chart with mathematical modelling of the proposed OWOA algorithm

(2017) where computational time is reduced during optimization process by adopting parallel computing technique. Patwal et al. (2018) introduced time-varying acceleration coefficient PSO-based mutation technique to analyse solar-based pump storage HTS system where different mutation techniques have been adopted to update the local best solutions. Ji et al. (2021) applied an enhanced Borg algorithm framework on wind-based HTS system and analysed the system energy performances under different dispatch scenarios where the designed evolution framework enhanced the convergence capability. Paul et al. (2020) successfully implemented chaotic whale optimization algorithm (WOA) (CWOA) on wind-based combined heat and power economic dispatch problem (CHPED) for economic operation. Wei et al. (2019) introduced mixed integer linearization technique, by which nonlinearity due to wind and solar unit for practical power system has been overcome.

For interconnected power system, Wang et al. (2018) designed a model of complimentary operation using hydro–thermal–wind–solar to increase the power generation efficiency and to reduce the thermal power fluctuation. The scarcity of water during summer season yields power generation problem by hydro-power unit in independent regional grid to provide the load demand. A scheduling of CHPED with wind- and solar-based renewable energy sources for fuel cost minimization was proposed by Paul et al. (2021a) and analysed the problem with a new optimization technique, quasi oppositional-based WOA (QOWOA), to deal with the

Table 1 Comparison of optimization results obtained for the unimodal, multimodal and fixed-dimensional multimodal benchmark functions

Function	OWOA		WOA		PSO		GSA		DE		FEP		GWO	
	Mean	Std	Mean	Std	Mean	Std	Mean	Std	Mean	Std	Mean	Std	Mean	Std
F_1	1.58E−86	3.75E−86	5.52E−74	1.57E−73	1.36E−04	2.02E−04	2.53E−16	9.67E−17	8.20E+14	5.90E−14	5.70E−04	1.30E−04	1.31E−04	1.99E−04
F_2	1.77E−63	3.01E−63	8.26E−52	1.77E−51	0.0421	0.0454	0.0556	0.1941	1.50E−09	9.90E−10	8.10E−03	7.70E−04	0.0401	0.0421
F_3	5.05E+04	2.28E+04	4.35E+04	1.47E+04	70.1256	22.1192	896.534	318.955	6.80E−11	7.40E−11	0.016	0.014	68.5623	19.2911
F_4	54.741	24.8159	56.2981	25.3395	1.0864	0.317	7.3548	1.7414	0	0	0.3	0.5	1.0532	0.276
F_5	27.6537	0.4816	28.0165	0.4769	96.7183	60.1156	67.5431	62.2253	0	0	5.06	5.87	93.3871	58.7634
F_6	0.4111	0.1502	0.3765	0.2166	1.02E−04	8.28E−05	2.51E−16	1.74E−16	0	0	0	0	0.99E−04	7.36E−05
F_7	3.40E−04	4.97E−04	0.005	0.0073	0.1228	0.0449	0.0894	0.0434	0.0046	0.0012	0.1415	0.3522	0.1133	0.0387
F_8	− 1.23E+04	567.1264	− 1.05E+04	1.76E+03	− 4.84E+03	1.15E+03	− 2.82E+03	493.037	− 1.10E+04	574.7	− 1.20E+04	52.6	− 4.28E+03	1.02E+03
F_9	0	0	0	0	46.7042	11.6293	25.9684	7.47	69.2	38.8	0.046	0.012	44.5456	10.3962
F_{10}	4.80E−15	2.62E−15	3.30E−15	1.98E−15	0.276	0.509	0.0621	0.2362	9.70E−08	4.20E−08	0.018	0.0021	0.258	0.498
F_{11}	0	0	0	0	0.0092	0.0077	27.7051	5.0403	0	0	0.016	0.022	0.0073	0.0064
F_{12}	0.016	0.0084	0.0191	0.0106	0.0069	0.0263	1.7996	0.9511	7.90E−15	8.00E−15	9.20E−06	3.60E−06	0.0058	0.0244
F_{13}	0.6294	0.2632	0.4841	0.2029	0.0067	0.0089	8.8991	7.1262	5.10E−14	4.80E−14	1.60E−04	7.30E−05	0.0059	0.0078
F_{14}	1.9904	0.9353	2.2612	2.0876	3.6271	2.5608	5.8598	3.8313	0.998	3.30E−16	1.22	0.56	3.4382	2.6221
F_{15}	5.55E−04	1.46E−04	6.40E−04	3.94E−04	5.77E−04	2.22E−04	3.67E−03	0.0016	4.50E−14	3.30E−04	5.00E−04	3.20E−04	5.63E−04	2.18E−04
F_{16}	− 1.03162	1.04E−09	− 1.03162	1.99E−09	− 1.03163	6.25E−16	− 1.03163	4.88E−16	− 1.03163	3.10E−13	− 1.03	4.90E−07	− 1.04052	5.18E−16
F_{17}	0.3979	4.17E−06	0.3978	5.48E−06	0.3978	0	0.3978	0	0.3978	9.90E−09	0.398	1.50E−07	0.4163	0
F_{18}	3.0001	3.12E−04	3	1.15E−04	3	1.33E−15	3	4.17E−15	3	2.00E−15	3.02	0.11	2.96	1.25E−15
F_{19}	− 0.3005	0	− 0.3004	1.70E−16	− 3.8627	2.58E−15	− 3.8627	2.29E−15	NA	NA	− 3.86	1.40E−05	− 3.7654	2.42E−15
F_{20}	− 3.2078	0.086	− 3.2302	0.1283	− 3.2663	0.0605	3.3177	0.0231	NA	NA	− 3.27	0.059	− 3.1888	0.0586
F_{21}	− 10.1518	0.0018	− 8.6196	2.5312	− 6.8651	3.0196	− 5.9551	3.7371	− 10.1532	2.50E−06	− 5.52	1.59	− 6.7542	3.0232
F_{22}	− 10.4018	0.0012	− 7.5087	3.1496	− 8.4565	3.087	− 9.6844	2.0141	− 10.4029	3.90E−07	− 5.53	2.12	− 8.5123	3.072
F_{23}	− 10.5353	0.0012	− 7.3929	3.4287	− 9.9529	1.7827	− 10.5364	2.60E−15	− 10.5364	1.90E−07	− 6.57	3.14	− 9.9498	1.7799

Table 2 Comparison of optimization results obtained for the composite benchmark functions

Function	OWOA		WOA		PSO		GSA		DE		CMA-ES		GWO	
	Mean	Std	Mean	Std	Mean	Std	Mean	Std	Mean	Std	Mean	Std	Mean	Std
F_{24}	56.8604	66.4073	150.5646	102.4002	100	81.65	6.63E−17	2.78E−17	6.75E−02	1.11E−01	100	188.56	100	80.23
F_{25}	205.5622	100.2621	192.3626	95.5703	155.91	13.176	200.6202	67.7208	28.759	8.6277	161.99	151	154.45	12.163
F_{26}	450.7415	115.7791	441.4643	177.0612	172.03	32.769	180	91.8936	144.41	19.401	214.06	74.181	171.22	31.653
F_{27}	507.353	95.5768	607.4306	138.5145	314.3	20.066	172	82.3276	324.86	14.784	616.4	671.92	309.4	20.059
F_{28}	147.5041	82.3309	132.8202	76.9266	83.45	101.11	200	47.1404	10.789	2.604	358.3	168.26	81.77	100.42
F_{29}	770.6224	180.259	795.4606	192.5481	861.42	125.81	142.0906	88.8714	490.94	39.461	900.26	8.32E−02	860.33	124.72

nonlinearity of solar radiation, wind speed and valve point loading of thermal units. Again, Paul et al. (2021b) enhanced their research by incorporating electric vehicles with wind–solar-based CHPED to minimize the use of thermal units during load demand. Liu et al. (2019) made a scheduling of hydro–wind–solar battery in independent grid to overcome the risk of hydropower generation during summer season.

A mathematical model of long-term hydro–wind-photovoltaic was designed by Yin et al. (2019) to increase the efficiency of power output and to reduce the standard deviation of the system. Zhao et al. (2019) developed a model to integrate the wind with solar where uncertainties of the system have been reduced and efficiency of power output has been increased. A modified differential evolution (MDE) algorithm was applied on hydro–wind–solar-based micro-grid system by Shu et al. (2019). The applied modified technique increases the global searching ability, and effective saving in cost is noted. In 2019, a multi-objective wind- and solar-based HTS problem has been analysed using nonlinear technique by Gul et al. (2019). The scheduled system of this work consists of four hydro reservoirs, three thermal units, one wind and one solar unit where contribution of renewable sources has been shown by reducing the impact of emission on environment while fulfilling the energy demand.

It has been observed from literature review that there are still some gaps in the research work. Most of these optimization techniques are suffering from local optima problems and less convergence speed and are taking more computational time resulting in less satisfactory results. Besides, the reviewed algorithms may give faithful results in other areas but not for higher nonlinearity-based problems.

In this article, the authors have incorporated wind and solar power with HTS system considering the transmission losses. The proposed system is composed of four hydro units, three thermal units, two wind and two solar units. The presence of uncertain behaviour of renewable sources and transmission losses of the system has made the system more nonlinear. The authors have used Weibull PDF (Genc et al. 2005) and PEM (Li et al. 2013) for analysing the uncertainty of the wind as well as the solar power. The authors have proposed a new heuristic technique opposition-based WOA (OWOA) (Wang et al. 2019) on HTS as well as in hydro–thermal–wind–solar scheduling (HTWSS) system to demonstrate the performances of the proposed algorithm on higher-order nonlinear system configuration. The proposed OWOA is developed being inspired from Wang et al. (2019). It is based on opposition-based learning (OBL) approach which enhances the searching behaviour of the basic WOA. In 2016, Mirjalili and Lewis (2016) developed a smooth and powerful optimization technique (*i.e.* WOA) which is based on searching behaviour of humpback whales. OBL has been developed by Rahnamayan et al. (2008) where opposite values are taken for each recommended value for searching of better solution. Different types of control variables are designed to judge the feasibility of the optimization technique. Initially, the superiority of the proposed algorithm has been investigated through twenty-nine benchmark functions. Later, the performance of the proposed algorithm has been investigated for conventional HTS problem and comparative study with other optimization techniques is made. Finally, the effects of renewable sources have also been discussed to obtain optimal solution using the proposed OWOA. Pros and cons of the proposed OWOA algorithm compared to aforesaid multi-objective algorithm are illustrated below:

- The SCA (Dasgupta et al. 2020) offered the best solution for the multi-objective HTS system with nonlinearity. But it manifests a slower convergence rate when settling towards the local optimal for solving challenging optimization tasks (Wang and Lu 2021). The suggested OWOA algorithm has better capability in dealing with nonlinear problems and offers a substantially faster convergence rate.
- One major advantage of KHA (Mukherjee and Mukherjee 2015) is that it needs a very few control variables in comparison with other optimization methods but for solving multimodal functions, it may often fail to find the best solution for solving multimodal functions. Better searching ability of the proposed OWOA algorithm forces it to provide optimal solution for unimodal and multimodal functions.

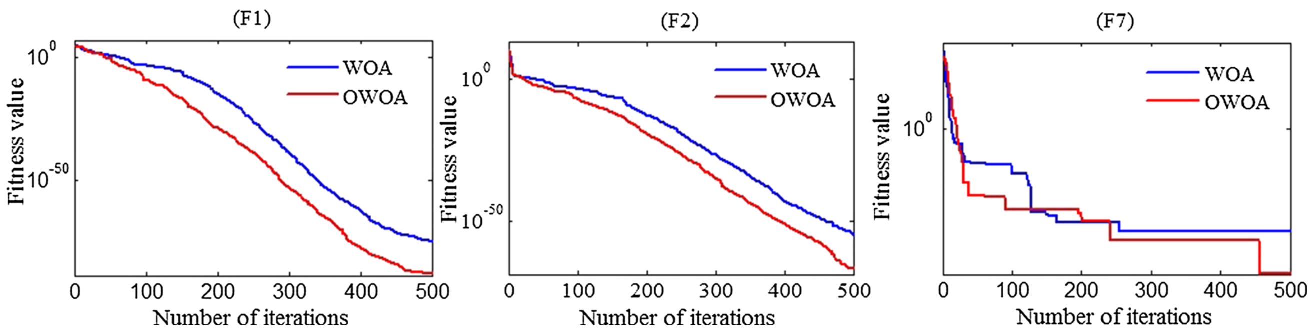

Fig. 3 Convergence profile for unimodal benchmark functions F1, F2 and F7

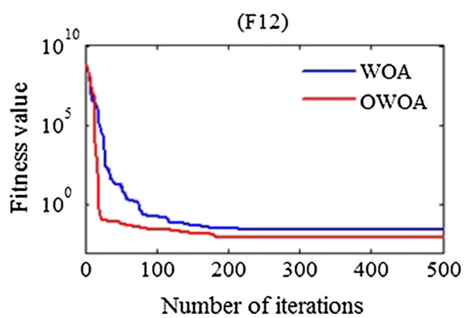

Fig. 4 Convergence profile for multimodal (F12) benchmark function

- It has been proved that most of the time NSGA-II approach (OuYang et al. 2008) offers much better quality solutions and yields better convergence mobility near the true Pareto-optimal than the other Pareto-optimal methods. But there are also disadvantages to restrict the spread of uniformity in some problems. MOPSO (Li et al. 2021) algorithm faces the difficulty of premature and insufficient diversity due to the selection of inappropriate leaders and inefficient evolution strategies. The different strategies involved in the proposed OWOA help to overcome the premature convergence of the basic WOA counterpart.
- NSGA-II-MOPSO approach satisfactorily balances the exploitation and the exploration task. But it suffers from low computational efforts while solving economic and micro-grid power dispatch problems (Dhiman 2020). However, the proposed OWOA optimization technique requires less number of iterations, so the required computational time requirement is less to perform the test.
- MOMVO (Aljarah et al. 2021) approach performs satisfactorily in maintaining and improving the coverage of Pareto-optimal solutions. But, it suffers from local optimality. Similarly, it is noted that MFO (Zhang et al. 2016) converges quickly but is easy to trap into local optimum. The success of the proposed OWOA algorithm is its ability to avoid stagnation.

The present authors are inspired to implement this new OWOA optimization technique in HTS and HTWSS system for the following advantages of OWOA.

- The OWOA technique is free from input control parameters.
- OWOA technique is much robust for different test systems with variable load profile.
- Less number of iterations is required to obtain global solution.
- Tuning capability is much better for OWOA technique.
- It exhibits high dealing capacity with nonlinear solutions.
- It makes a strong balance between the global exploration and the local exploitation.
- Convergence rate is much faster.
- Less CPU time is required to perform the test.

The foremost contributions of this paper are mentioned below:

- In present work, few suitable unimodal, multimodal, composite benchmark functions have been chosen to verify the efficacy of the proposed approach. Moreover, three different test studies of non-renewable and renewable (wind and solar)-based HTS have been investigated for solving single and multi-objective functions.
- The overall energy production cost and fuel emission are minimized while considering the uncertainty of the parameters along with maximum utilization of renewable energy sources.
- An optimal scheduling of hydro, thermal, wind and solar has been implemented on the prescribed energy market guidelines.
- Introduced an efficient optimization technique, named as OWOA, to deal with different uncertainties of the proposed system.
- The obtained results on two test systems are reported and compared the results obtained with the other state-of-the-art algorithms reported in this field to judge its superiority.

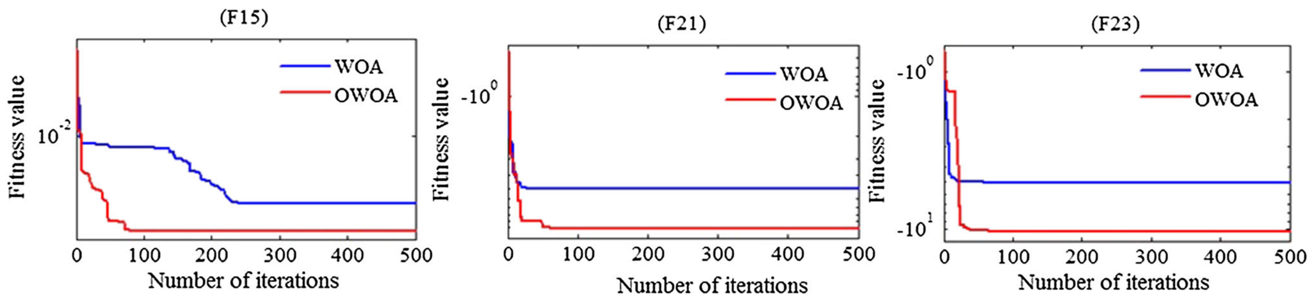

Fig. 5 Convergence profile for fixed-dimensional multimodal benchmark functions F15, F21 and F23

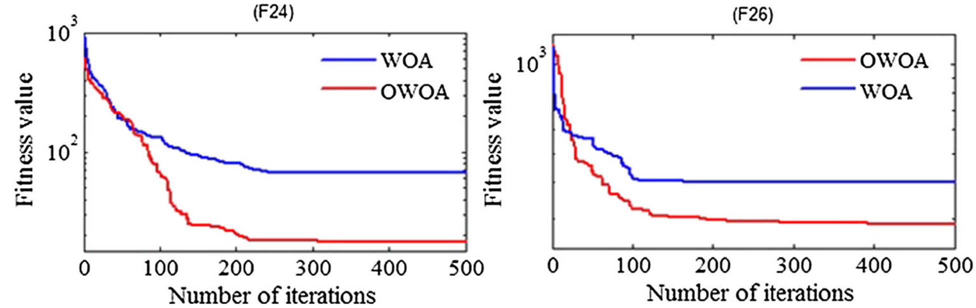

Fig. 6 Convergence profile for composite benchmark functions F24 and F26

Table 3 Hourly water discharge of hydro reservoirs and power generation by thermal units obtained by OWOA pertaining to ELS with loss

Hour	Discharge of hydro reservoir ($m^3 \times 10^5$)				Thermal power (MW)			Thermal cost ($/h)	Emission (lb/h)
	Q_{h1}	Q_{h2}	Q_{h3}	Q_{h4}	P_{Th1}	P_{Th2}	P_{Th3}		
1	1.0881	0.9035	2.0589	1.3682	101.5277	209.8158	50	1277.622	355.7579
2	0.5015	0.6	1.8201	1.3241	101.5304	124.9079	229.5196	1504.466	682.8146
3	1.0066	0.6314	2.4998	0.9043	162.2831	124.9079	139.7598	1550.333	417.6311
4	0.5786	0.6667	1.8818	1.0028	101.1382	124.9079	139.7598	1267.576	323.546
5	0.813	0.8075	1.3787	0.6816	102.6685	124.9079	139.7598	1262.4	324.8514
6	0.5	0.6	1.0944	1.7382	174.9983	124.9079	140.0398	1527.655	449.3659
7	0.6703	0.6014	2.3862	0.6468	174.999	209.8158	319.2793	2250.995	1579.636
8	0.5	1.0602	1.1913	1.5288	174.9916	124.9079	319.2794	2025.609	1390.237
9	0.8193	0.947	1.4566	1.1023	102.6789	209.8158	409.0392	2274.996	2346.784
10	0.5	0.6	2.6671	1.4229	166.1186	294.7237	319.2794	2510.902	1903.972
11	1.0662	0.8486	1.0191	1.053	102.6718	294.7237	319.2794	2228.223	1802.301
12	0.5	0.6588	2.0973	0.8179	163.8818	294.7237	409.0392	2800.823	2789.593
13	0.7321	0.7895	1.3526	0.6	174.9999	209.8166	409.0392	2537.556	2470.495
14	1.1206	1.1395	1.7248	1.6931	20.6996	209.8158	319.2794	1779.673	1457.964
15	0.6468	0.6709	1.4504	1.0709	102.6785	124.9079	409.0392	2049.585	2157.404
16	0.5	0.6	1.0838	1.9257	97.0537	209.8158	319.2794	2007.185	1451.387
17	0.6287	0.8862	1.6536	1.384	102.6647	209.8158	319.2794	1988.421	1455.918
18	1.0248	1.1163	1.036	1.7953	102.6762	209.8158	319.2794	1988.416	1455.928
19	1.0029	0.7585	2.1663	1.7352	102.6713	209.8158	319.2794	1988.399	1455.924
20	0.8395	0.8049	1.5574	1.3318	102.6691	209.8158	319.2794	1988.406	1455.922
21	1.0366	0.8144	1.917	1.5161	20.002	124.9029	319.2794	1548.302	1269.214
22	1.1191	1.3026	1.4091	1.6775	21.625	209.8158	139.7598	1287.007	515.4451
23	1.0617	0.8922	1.5468	1.9357	102.6724	209.8158	50	1273.749	356.7393
24	1.2436	1.4999	1.4809	2	22.5572	124.9079	139.7598	1069.582	325.248
Fuel cost ($/day)						43988			
Emission (lb/day)						30194			

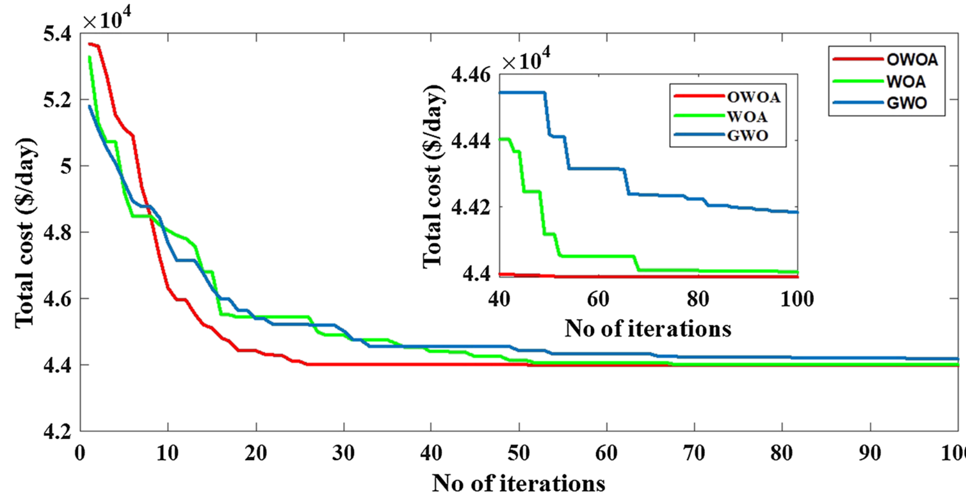

Fig. 7 Cost convergence graph of HTS with loss system using different algorithms

Table 4 Comparison of generation cost of ELS-based results for 4-hydro and 3-thermal system with loss obtained by different algorithms

Algorithms	Fuel cost ($/day)			Computational (s)
	Best	Average	Worst	
OWOA	43,988	44,028	45,012	18.1
WOA	44,002	44,042	44,124	27.8
GWO	44,182	44,032	44,108	38.6
QEA Wang et al. (2012)	44,686	–	–	–
SPSO Zhang et al. (2011)	44,980	–	–	–
DE Mandal and Chakraborty (2009)	44,526	–	–	–
Fuzzy EP Basu (2004)	45,063	–	–	–

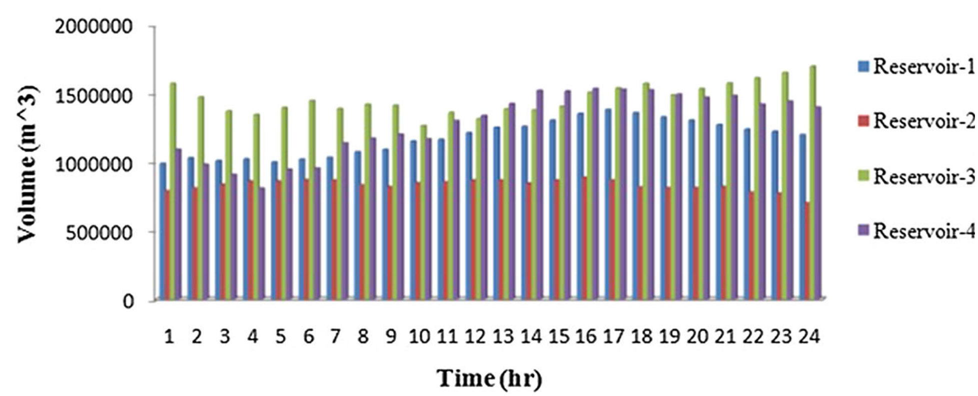

Fig. 8 Reservoir volume of hydro units for ELS of HTS with loss

The rest of the paper is organized as follows. Problem formulation of the test systems is explained in Sect. 2. The different optimization algorithms are elaborated in Sects. 3 and 4. Test systems and simulation results are presented and discussed in Sect. 5. Finally, the conclusions of the present research work are drawn in Sect. 6 while indicating some potential future research direction.

2 Problem formulation

Schematic model of wind and solar sources incorporated to HTS problem is illustrated in Fig. 1. Due to the presence of some practical situation, the complexity and the nonlinearity of the problem became more. Some presumptions have been taken into consideration and applied to both the test systems to solve this complex nonlinear problem.

Table 5 Hourly water discharge of hydro reservoirs and power generation by thermal units obtained by OWOA pertaining to EES with loss

Hour	Discharge of hydro reservoir ($m^3 \times 10^5$)				Thermal power (MW)			Thermal cost ($/h)	Emission (lb/h)
	Q_{h1}	Q_{h2}	Q_{h3}	Q_{h4}	P_{Th1}	P_{Th2}	P_{Th3}		
1	0.8332	0.6	1.7384	1.24	143.719	145.1217	98.0113	1806.083	315.1515
2	0.826	0.6272	2.0234	0.6292	174.9998	187.6101	138.9953	1825.279	573.1663
3	0.6374	0.6	2.6926	0.8158	163.4239	171.8708	117.8172	1933.795	451.7174
4	0.568	0.6	2.3561	1.7856	128.8366	124.9323	83.5011	1515.472	233.6429
5	0.9028	0.6	2.548	0.6	158.2707	164.8387	112.5234	1932.068	412.5663
6	0.8174	0.7032	2.0535	0.7263	174.9877	213.3972	130.037	1826.433	622.3428
7	0.8931	0.6181	1.2882	1.4325	174.995	208.0085	181.3803	2063.637	773.1366
8	0.5457	0.6304	2.7925	1.9192	174.982	187.6276	293.4316	2401.68	1323.418
9	0.9918	0.7045	1.4605	1.0089	174.9997	214.1442	336.2613	2455.932	1733.273
10	1.0263	0.7603	1.1162	1.9944	174.9966	248.07	198.7491	2364.433	983.0181
11	0.8025	0.9268	2.3656	1.3919	174.9983	268.9249	288.0331	2646.896	1568.569
12	1.1238	0.8002	1.3296	1.5445	174.9976	217.2641	315.4194	2335.597	1572.511
13	0.9093	0.8215	1.0512	1.8893	174.9962	187.6099	287.0304	2406.185	1278.898
14	0.8289	0.8548	2.0239	1.7235	174.9957	193.6065	235.7092	2106.378	982.7629
15	1.0091	0.8714	1.2181	1.1468	174.977	187.6331	226.6577	2072.12	919.5854
16	0.7078	0.9519	1.9027	1.8219	174.9805	187.6668	253.0008	2272.803	1063.522
17	0.906	0.9771	1.5707	1.439	174.9957	187.5938	250.9837	2257.165	1051.67
18	0.9487	1.0089	2.7598	1.5209	174.9806	187.5875	358.5028	2640.889	1858.493
19	0.7277	1.0656	1.576	1.656	174.9542	192.3434	263.5413	2331.936	1138.883
20	0.8702	1.1387	1.3141	1.8819	174.985	187.6698	215.5752	2115.188	864.8717
21	0.8433	1.1269	1.0566	1.8275	159.9168	167.1757	114.363	1934.981	425.3583
22	0.697	1.0101	1.0894	1.8659	144.8214	146.6603	99.1562	1822.135	322.0955
23	0.5837	1.0927	1.1407	2	142.1166	142.951	96.4578	1781.74	305.5567
24	0.5003	1.1097	1.1657	2.0001	131.0555	128.0364	85.7422	1567.87	244.9535
Fuel cost ($/day)					50416.69				
Emission (lb/day)					21019.16				

Table 6 Comparison of emission for EES results for 4-hydro and 3-thermal system with loss obtained by different algorithms

Algorithms	Emission (lb/day)			Computational (s)
	Best	Average	Worst	
OWOA	21,019.16	21,055.39	21,787.43	19.12
WOA	21,038.46	21,068.56	21,815.17	31.84
GWO	21,259.73	21,238.72	22,016.69	43.78

2.1 Objective function

The main objective of this presentation is to minimize generation cost as well as emission to make the system more economical with pollution free. In this research work, both single- and multi-objective functions are dealt with to achieve the reliable operation of the power system while fulfilling all the constraints.

2.1.1 Single-objective function

2.1.1.1 Cost minimization The cost function of fuel for HTWSS is represented as in (1).

$$\left\{\begin{aligned} &\text{Minimized } C_{\text{total}} \\ &\quad = \sum_{i=1}^{N_{th}} \sum_{t=1}^{T_l} \Big(\alpha_{\text{Thi}} (P_{\text{Thi}}^t)^2 + \beta_{\text{Thi}} P_{\text{Thi}}^t + \gamma_{\text{Thi}} \\ &\qquad + \left| \delta_{\text{Thi}} \sin(\varepsilon_{\text{Thi}} \times (P_{\text{Thi}}^{\min} - P_{\text{Thi}}^t)) \right| \Big) \\ &\qquad + \sum_{m=1}^{N_w} \sum_{t=1}^{T_l} \left(E_{o,m}^t + E_{u,m}^t \right) + \sum_{k=1}^{N_s} \sum_{t=1}^{T_l} F\left(P_{S,k}^t\right) \end{aligned}\right. \tag{1}$$

In the above equation, C_{total} represents the total cost, whereas P_{Thi}^t is the thermal ****power generation at time t. Time (t) is taken for each hour interval in a day, t = 1,2,3,...,24, and i varies from 1 to 3. The total number of thermal units is denoted as N_{th}, and T_l shows at 24th hour. $P_{\text{Thi}}^{\min}$ is the minimum thermal power generation. Here, α_{Thi}, β_{Thi},γ_{Thi} are the cost coefficients and δ_{Thi}, ε_{Thi} are the coeffi-

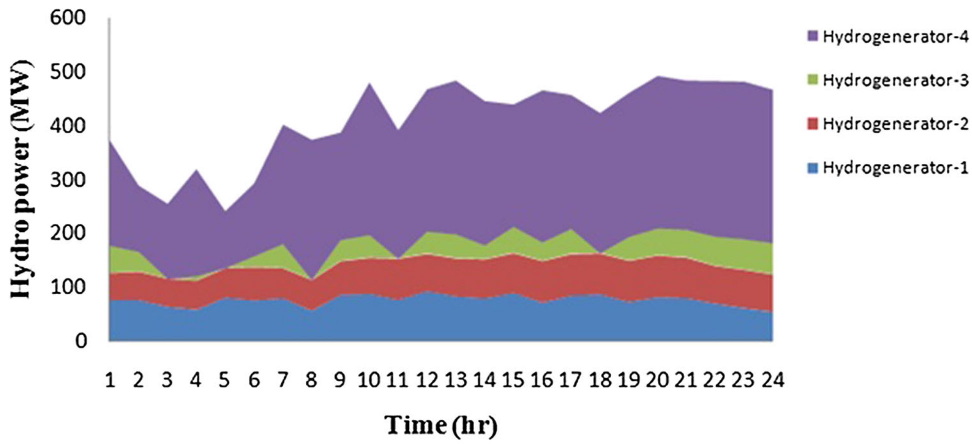

Fig. 9 Hydropower generation for EES of HTS with loss

cients of the valve point loading. In (1), N_s is total number of solar unit and P^t_{Sk} depicts the solar power generation at time t. The actual cost function of thermal power plant should not be a linear function due to the presence of different input output characteristics of multi-valve steam turbine. N_w is the total number of wind units. $E^t_{o,m}$ and $E^t_{u,m}$ represent, respectively, the overestimation cost and the underestimation cost of wind power plant for time t. $F\left(P^t_{S,k}\right)$ represents solar cost of solar power plant for time t. The uncertainty of wind speed may be reduced while using Weibull probability distribution function (PDF) (Genc et al. 2005). The brief introduction of overestimation cost and underestimation cost of wind power plant is illustrated below.

When the actual generated wind energy is less than the expected wind energy, it is defined as overestimation wind cost. As a result, there is a deficiency of power to fulfil the demand of the load. That demand can be fulfilled by using a spinning reserve. The overestimation cost of wind generated power is defined as follows.

$$\begin{cases} E^t_{o,m} = C_{o,m} \times W^t_m \\ \left[1 - \exp\left(-\left(\frac{V_{in,m}}{c_m}\right)^{l_m}\right) + \exp\left(-\left(\frac{V_{out,m}}{c_m}\right)^{l_m}\right)\right] \\ + \left(\frac{W_{R,m}V_{IN,m}}{V_{R,m}-V_{IN,m}} + W^t_m\right) \\ \left[\exp\left(-\left(\frac{V_{in,m}}{c_m}\right)^{l_m}\right) - \exp\left(-\left(\frac{V_{in,m}+W^t_m\frac{V_{R,m}-V_{IN,m}}{W_{R,m}}}{c_m}\right)^{l_m}\right)\right] \\ + \frac{W_{R,m}c_m}{V_{R,m}-V_{IN,m}} \\ \left[\zeta\left(1+\frac{1}{l_m}, \left(\frac{V_{in,m}+W_{m,t}\frac{V_{R,m}-V_{IN,m}}{W_{R,m}}}{c_m}\right)^{l_m}\right)\right. \\ \left. -\zeta\left(1+\frac{1}{l_m}, \left(\frac{V_{IN,m}}{c_m}\right)^{l_m}\right)\right] \end{cases} \tag{2}$$

The underestimation cost of wind generated power is defined, when the actual power in wind generated power plant is more with respect to the planned value of wind generated power. This extra energy requires balancing in the system. Otherwise, this excess electrical energy will be washed out. Underestimation cost is represented by (3)

$$\begin{cases} E^t_{u,m} = c_{u,m} \times \left(W_{R,m} - W^t_m\right) \\ \left[\exp\left(-\left(\frac{V_{R,m}}{c_m}\right)^{l_m}\right) - \exp\left(-\left(\frac{V_{out,m}}{c_m}\right)^{l_m}\right)\right] \\ + \left(\frac{W_{R,m}V_{IN,m}}{V_{R,m}-V_{IN,m}} + W^t_m\right) \\ \left[\exp\left(-\left(\frac{V_{R,m}}{c_m}\right)^{l_m}\right) - \exp\left(-\left(\frac{V_{in,m}+W_{m,t}\frac{V_{R,m}-V_{IN,m}}{W_{R,m}}}{c_m}\right)^{l_m}\right)\right] \\ + \frac{W_{R,m}c_m}{V_{R,m}-V_{IN,m}} \\ \left[\zeta\left(1+\frac{1}{l_m}, \left(\frac{V_{in,m}+W_{m,t}\frac{V_{R,m}-V_{IN,m}}{W_{R,m}}}{c_m}\right)^{l_m}\right)\right. \\ \left. -\zeta\left(1+\frac{1}{l_m}, \left(\frac{V_{R,m}}{c_m}\right)^{l_m}\right)\right] \end{cases} \tag{3}$$

where $E^t_{o,m}$ denotes the cost of overestimation and $E^t_{u,m}$ denotes the underestimation cost of the mth wind for time t; $c_{o,m}$, $c_{u,m}$ are, respectively, the cost coefficients of overestimation and underestimation; $W_{R,m}$ and $V_{R,m}$, in order, represent output of rated power as well as rated wind velocity; the cut in speed ($V_{in,m}$) and speed of cut out ($V_{out,m}$) are the range of wind speed in which wind turbines can generate the power; and I_m and c_m are, in sequence, the shape factor and the scale factor.

The concept of solar power generation $\left(F\left(P^t_{Sk}\right)\right)$ cost is represented as under.

$$F\left(P^t_{Sk}\right) = \text{PUC}^t_{S,k} \times P^t_{S,k} \times D^t_{S,k} \tag{4}$$

where $\text{PUC}^t_{S,k}$ is the per unit cost of the kth solar unit at tth hour; P^t_{Sk} represents total solar power; and $D^t_{s,k}$ is the status of solar plant (1 for on state and 0 for off state.

The generation of solar power mostly depends on intensity, temperature and irradiance of sunlight. Therefore, solar

Table 7 Hourly water discharge of hydro reservoirs and power generation by thermal units obtained by OWOA pertaining to CEES

Hour	Discharge of hydro reservoir ($m^3 \times 10^5$)				Thermal power (MW)			Thermal cost ($/h)	Emission (lb/h)
	Q_{h1}	Q_{h2}	Q_{h3}	Q_{h4}	P_{Th1}	P_{Th2}	P_{Th3}		
1	0.5088	0.6	1.5424	1.0234	160.3996	124.9079	139.7598	1551.996	413.3992
2	0.9714	0.8584	1.9018	1.5038	126.7395	124.9079	139.7598	1454.733	352.3302
3	0.5978	0.6	1.5565	0.7017	160.5255	124.9079	139.7598	1551.905	413.6795
4	0.7183	0.9184	2.8255	0.9959	109.5428	124.9079	139.7598	1322.255	331.3614
5	0.952	0.6003	2.4058	0.7563	146.6104	124.9079	139.7598	1542.392	385.0933
6	0.6239	0.6	1.8332	1.7324	102.6734	205.5344	138.9835	1507.953	499.1784
7	0.6571	0.7933	2.1477	1.4018	174.9978	124.9119	323.6091	2069.088	1424.986
8	0.8927	0.8714	2.7164	1.6639	174.9999	209.8166	270.7404	2304.472	1234.028
9	0.9748	0.8496	1.217	1.3618	174.9986	256.8617	270.2998	2611.278	1399.351
10	1.2449	0.8031	1.0916	1.8897	175	239.996	230.0798	2239.44	1101.626
11	1.2037	0.7168	2.8078	1.312	174.9994	222.3487	354.4482	2663.95	1922.737
12	1.3778	0.7704	2.2727	1.3569	174.9931	289.297	307.7792	2554.355	1808.639
13	1.1621	1.0371	1.8122	1.248	174.9991	209.818	321.5072	2273.414	1597.426
14	0.6818	0.9056	1.2529	1.637	174.9928	124.9079	309.8763	2061.624	1317.146
15	0.6628	0.7296	1.3325	1.7154	174.999	264.8259	139.7598	2065.05	839.9761
16	0.6823	0.7876	1.9736	1.5613	174.9924	273.6771	198.2261	2386.105	1089.894
17	0.5895	0.6787	1.18	1.0394	174.9946	209.8158	294.0291	2329.378	1390.232
18	0.6509	0.7519	1.4333	1.3021	174.9933	227.6365	311.9319	2438.902	1579.901
19	0.6689	0.7584	1.6773	1.9714	174.9993	242.125	200.8403	2335.596	969.3314
20	0.8092	1.0482	1.0035	1.1954	174.9998	209.8208	241.5804	2104.445	1061.313
21	0.978	0.704	1.076	1.6705	174.9993	124.9109	146.9066	1592.603	469.6328
22	0.6531	1.4253	1.2287	2	104.6612	124.9109	139.7598	1279.849	326.6339
23	0.718	1.3782	1.2828	1.8683	102.6739	124.7685	139.7598	1262.958	324.6518
24	0.5202	1.0137	1.3034	1.7553	102.6869	124.9079	133.4695	1290.39	307.3814
Fuel cost ($/day)					43988				
Emission (lb/day)					30194				

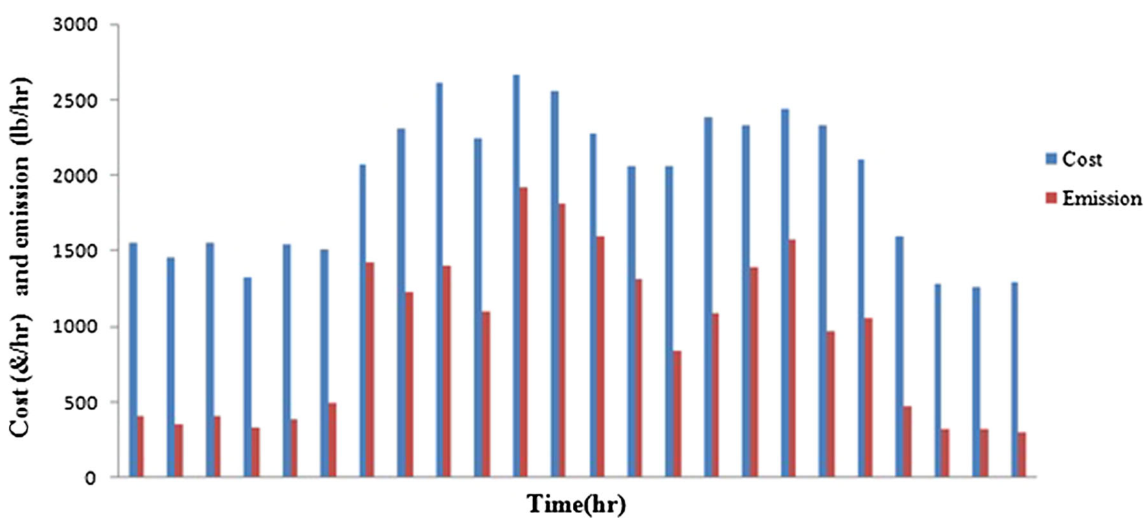

Fig. 10 Cost and emission of thermal units for CEES of HTS with loss

Table 8 Comparison of generation cost (CEES) results for 4-hydro and 3-thermal system with loss obtained by the proposed method and other methods

Algorithms	Fuel Cost ($/day)	Emission (lb/day)	Computational time (s)
OWOA	46794.13	22559.92	28.34
WOA	46825.69	22567.38	47.76
GWO	47067.34	22709.67	74.39
Fuzzy EP Basu (2004)	47906	26234	45.82

power of kth unit at tth hour due to intensity and temperature is represented by (5):

$$P_{Sk}^{t} = P_{Skr} \times \frac{I_k(t)}{I_{kr}} [1 + c(T(t) - T_r)] \quad (5)$$

where P_{Skr} corresponds to the rated power of the kth solar panel in standard environment and c is the temperature coefficient of power, $I_k(t)$ and I_{kr} represent intensity of the sunlight and the rated intensity of sunlight at standard atmosphere, and T_r and $T(t)$ signify, in order, the rated temperature in a standard environment along with temperature at time t correspondingly.

2.1.1.2 Emission minimization The target for second single-objective function is to minimize the emission, without taking cost minimization into consideration. The mathematical representation of thermal plant emission (e_{th}) may be formulated as stated below in (6).

$$\text{Minimized}\, e_{Th} = \sum_{t=1}^{T} \sum_{i=1}^{N_{th}} \left[b_{i0} + b_{i1} P_{\text{Thi}}^{t} + b_{i2} (P_{\text{Thi}}^{t})^2 + b_{i3} \exp(b_{i4} P_{\text{Thi}}^{t}) \right] \quad (6)$$

In (6), b_{i0}, b_{i1}, b_{i2}, b_{i3} and b_{i4} denote emission coefficients, whereas P_{Thi}^{t} is the thermal power output.

2.1.2 Multi-objective function

Previously two single-objective functions (namely cost and emission) are minimized independently. But to judge the effectiveness of the proposed algorithm for multi-objective environment, both generation cost and emission are minimized simultaneously. A penalty factor (μ) has been used in the multi-objective function to bring the generation cost and emission into same priority level. The mathematical representation of the multi-objective function (F) is formulated in 7.

$$F = (\text{Minimized}\, C_{\text{total}}) + \mu\, (\text{Minimized}\, e_{th}) \quad (7)$$

Different values of penalty factor ($i.e.$ μ whose unit is taken as $\$/lb$) are assigned for different test studies to bring the generation cost and emission into the same priority level and its value in different case studies is as under:

- For Test sustem-1: $\mu = 2$ $ / lb
- For Test sustem-2: $\mu = 4$ $ / lb
- For Test sustem-3: $\mu = 4$ $ / lb

2.2 Constraints

The constraints associated with the problem are presented as follows:

2.2.1 Equality constraints

The equality constraints associated with the problem are power balance equation of power system, water dynamic balance equation of hydro unit, water discharge continuity equation of hydro unit, etc. The mathematical representation of equality constraints is discussed below.

2.2.1.1 Power balance equation In power balance equation, the total power generated by thermal, hydro, wind and solar provides total demand of load and transmission losses in the system formulated in 8.

$$\sum_{i=1}^{N_{Th}} P_{\text{Thi}}^{t} + \sum_{j=1}^{N_H} P_{Hj}^{t} + \sum_{n=1}^{N_w} P_{wn}^{t} + \sum_{k=1}^{N_S} P_{sk}^{t} = P_d^t + P_{\text{Loss}}^{t}. \quad (8)$$

In the above relation, a total number of thermal units, hydro units, wind units and solar generating units are defined by N_{Th}, N_h, N_w and N_S, respectively; P_{Thi}^{t} and P_{wn}^{t} signify generation of power in thermal and wind unit for scheduling time t, respectively. Total load demand is defined by P_d^t and loss of the transmission line by P_{Loss}^{t} for t interval. The transmission loss at the tth hour P_{Loss}^{t} is formulated in (9)

$$P_{\text{Loss}}^{t} = \sum_{i=1}^{N} \sum_{j=1}^{N} P_i^t B_{ij} P_j^t \qquad \text{for } t = 1, 2, ..., T, \quad (9)$$

where $N = N_{Th} + N_H + N_W + N_S$.

In (8), P_{Hj}^{t} represents in hydro generation which is formulated by (10)

Table 9 Optimal results obtained by OWOA for ELS of wind–solar-based HTS system

Hour	Discharge of hydro reservoir ($m^3 \times 10^5$)				Thermal power (MW)			Wind Power (MW)		Solar panel on/off status of Plant 1	Solar panel on/off status of Plant 2	Solar Power (MW)	
	Q_{h1}	Q_{h2}	Q_{h3}	Q_{h4}	P_{Th1}	P_{Th2}	P_{Th3}	P_{w1}	P_{w2}			P_{s1}	P_{s2}
1	0.646	0.7043	2.6388	0.8919	102.7	125.13	229.65	0.44	20.24	1111011010000	0110001000011	0	0
2	1.2509	0.8957	1.5501	1.1245	32.61	209.81	139.63	3.01	17.87	1011011111011	1111001010100	0	0
3	0.5	1.0238	1.7206	0.9637	102.67	124.9	135.97	3.61	20.75	0011110100100	1001011001111	0	0
4	1.1941	1.0562	1.6	1.8659	29.36	42.59	139.76	15.39	20.53	1100110001010	1011010001100	0	0
5	0.6588	0.7192	1.5777	1.3815	102.66	124.86	57.26	17.24	18.94	1110111111111	1111111111111	2.18	2.34
6	0.6804	0.6449	1.0052	0.9092	22.53	209.81	139.69	14.51	20.04	1111111111111	1111111111111	43.77	43.77
7	0.6325	1.4032	1.4911	0.9419	103.32	125.77	230.16	2.98	15.6	1111001011101	0111001001011	73.34	58.43
8	0.7664	0.7277	1.0524	1.7805	20.01	126.81	139.76	0	17.6	1111101111010	0011101111010	170.61	146.99
9	0.982	0.6	2.0325	0.6344	102.94	122.22	232.6	0	7.96	0111011111010	1110111110111	157.85	188.4
10	1.1823	1.0201	2.028	1.9191	102.68	208.89	50	2.11	2.55	0000110011010	1010010101011	130.72	169.59
11	0.7586	1.026	2.2369	1.7929	20.3	126.14	98.9	15.71	16.81	0011011001011	1101000001110	250.9	199.7
12	0.6062	0.659	2.469	0.7985	102.67	124.91	229.51	2.65	3.66	0010110100110	0011001100101	223.38	223.38
13	0.5	0.8055	1.9386	0.6	22.18	40	120.22	13.37	19.89	1000111111111	1010111101101	342.97	290.57
14	0.8987	0.6358	1	1.6757	20	124.91	50.07	7.75	18.78	1110111011010	0011010101010	231.22	167.43
15	0.5487	0.6	2.2485	1.5702	102.68	124.35	127.67	0	13.85	0101010110010	1001010100011	143.45	140.04
16	1.1301	1.021	2.1166	1.5351	102.22	40	50	5.58	4	0111111111111	0101110001111	256.83	171.22
17	0.6055	0.6	1.7998	1.0041	174.98	211.21	50	27.16	23.42	1111110000110	1111111010111	90	132.25
18	1.2186	0.6986	1.8211	1.3845	102.72	40.54	409.26	10.95	4.11	1010101111111	0011001111111	70.77	66.72
19	0.7421	0.6522	1.006	1.7472	174.93	124.91	319.28	0	1.63	1101111010001	0110111001101	9.33	9.88
20	0.548	0.6059	1.0175	1.5648	174.6	245.65	138.02	84.06	1.13	0100101011101	0100010011100	0	0
21	0.6266	0.9075	1.2161	1.358	102.67	209.61	139.55	14.15	18.21	1101000101010	1111111100110	0	0
22	0.6251	1.1624	1.6721	1.7432	20	125.25	229.51	1.13	17.29	0111110011010	0001110000101	0	0
23	1.1142	0.6818	1.7388	1.8452	102.89	124.83	138.32	12.82	0	1010001110110	1001101001101	0	0
24	1.0842	1.3492	1.5608	1.9984	20.02	123.8	139.76	2.37	14.85	0111110111010	0101000111000	0	0
Fuel cost ($/day)										32,059.43			
Emission (lb/day)										12,782.32			
Solar cost ($/day)										1097.54			
Wind cost ($/day)										4041.72			

Table 10 Comparison of fuel cost for ELS of wind–solar-based HTS system

Algorithms	Fuel cost ($/day) Best	Average	Worst	Computational time (s)
OWOA	32,059.43	32,091.34	33,182.75	20.1
WOA	32,076.54	32,128.55	32,971.64	33.4
GWO	32,158.76	32,207.98	33,063.82	44.1
SCA Dasgupta et al. (2022)	37,755.14	–	–	27.6
BSA Dasgupta et al. (2022)	38,087.48	–	–	37.41

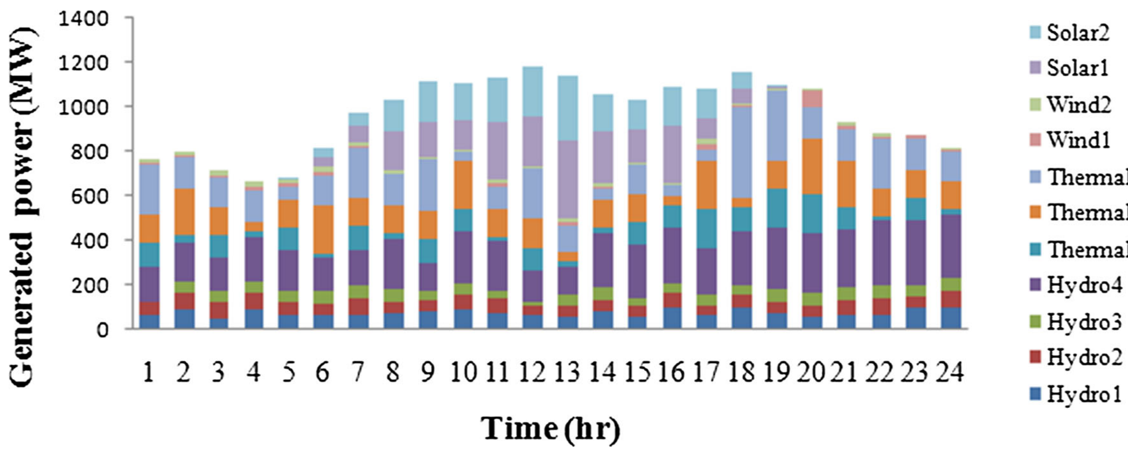

Fig. 11 Power generation by all units for ELS of HTWSS with loss

$$P_{Hj}^{t} = c_{1j}(v_{Hj}^{t})^{2} + c_{2j}(q_{Hj}^{t})^{2} + c_{3j}(v_{Hj}^{t}q_{Hj}^{t}) + c_{4j}v_{Hj}^{t} + c_{5j}q_{Hj}^{t} + c_{6j}, \quad (10)$$

where v_{Hj}^{t} and q_{Hj}^{t} are, respectively, volume and discharge of the jth hydro generator, and generation coefficients of the jth hydro-generator are c_{1j},c_{2j}, c_{3j},c_{4j}, c_{5j} and c_{6j}.

2.2.1.2 Water dynamic balance of the hydro reservoir unit The dynamic water balance of the hydro reservoir unit can be represented as in (11)

$$v_{Hj}^{t} = v_{Hj}^{t-1} + I_{Hj}^{t} - q_{hj}^{t} - S_{Hj}^{t} + \sum_{r=1}^{N_u}(q_{Hm}^{t-t_d} + S_{Hm}^{T_l-t_d}), \quad (11)$$

where I_{Hj}^{t} represents the inflow at the tth hour, q_{Hj}^{t} is the discharge at the tth hour, S_{Hj}^{t} is the spillage at the tth hour, v_{Hj}^{t} and v_{Hj}^{t-1} denote, respectively, the jth reservoir volume for tth and $(t-1)$th time interval, t_d represents transport delay of water, $q_{Hm}^{t-t_d}$ is the discharge of water after $(t-t_d)$, N_u denotes upstream plants on top of the jth hydro plant, and r varies from 1 to N_u upstream reservoir.

2.2.1.3 Water discharge continuity representation of hydro generator Water discharge continuity of hydro generator may be represented by (12).

$$q_{Hj}^{T} = v_{Hj}^{ini} - v_{Hj}^{fin} + \sum_{t=1}^{T_l} I_{t,Hj} - \sum_{t=1}^{T_l-1} q_{t,Hj} + \sum_{t=1}^{T_l}\sum_{m=1}^{N_u} q_{Hm}^{t-t_d}, \quad (12)$$

where q_{Hj}^{T} denotes last hydro unit discharge, and v_{Hj}^{ini} and v_{Hj}^{fin} are, respectively, reservoir first and last volume.

2.2.2 Inequality constraints

The inequality constraints associated with the problem are operating limits of thermal, hydro, wind and solar generators and volume and discharge limitation of reservoir.

2.2.2.1 Operating limits of the generators (a) Operating limits of the thermal generators may be stated in (13)

$$P_{\text{Thi,min}} \le P_{\text{Thi}}^{t} \le P_{\text{Thi,max}} \quad j = 1, 2, ..., N_{Th};\; t = 1, 2, ..., T_l, \quad (13)$$

where $P_{\text{Thi,min}}$ and $P_{\text{Thi,max}}$ indicate, in sequence, the least and the highest generation of power for the ith unit of thermal generator.

Table 11 Optimal results obtained by OWOA for EES of wind–solar-based HTS system

Hour	Discharge of hydro reservoir ($m^3 \times 10^5$)				Thermal power (MW)			Wind power (MW)		Solar panel on/off status of Plant 1	Solar panel on/off status of Plant 2	Solar power (MW)	
	Q_{h1}	Q_{h2}	Q_{h3}	Q_{h4}	P_{Th1}	P_{Th2}	P_{Th3}	P_{w1}	P_{w2}			P_{s1}	P_{s2}
1	0.9343	0.8042	1.5819	0.9058	106.1291	91.366	50	90	60	0111111010010	0110100111100	0	0
2	0.8301	0.7314	1.4737	1.4492	100.7583	91.8467	57.1335	90	60	1000011010111	1110011100010	0	0
3	0.683	0.684	1.9901	0.7174	110.8686	95.0147	67.4939	90	60	1000111011001	1000101101110	0	0
4	0.7625	0.6	1.7123	1.1192	81.2863	49.1146	50	90	60	0101110010101	1111111001001	0	0
5	0.6621	0.6	2.4222	1.7444	81.1128	65.2652	50	90	60	1111101101111	1110111111111	1.94	2.18
6	0.8083	0.868	1.3052	1.2547	89.4374	67.0008	52.3962	90	60	1111111111111	1111111111111	43.77	43.77
7	1.4412	0.6	1.3626	1.75	78.854	63.0891	50	90	60	1111111111111	1111111111111	109.4	109.4
8	0.7858	0.6	2.5006	1.1392	65.9643	57.2234	50	67.9252	42.0341	1111111111111	1011111111111	230.98	217.86
9	0.7298	0.6755	2.1299	0.6779	90.9031	80.4265	50	90	60	1111111111111	1111111111111	224.04	224.04
10	0.6012	0.6	1.512	0.9811	63.535	42.6818	50	31.1961	55.0223	1111110111011	1111011111110	257.91	261.44
11	1.1539	0.6	1.015	0.729	62.4149	41.4424	50	67.353	17.9927	0100110111100	0111011101001	256.02	276.51
12	0.6892	0.6	2.0922	1.9085	63.5694	40	50	30.5922	55.1343	0100101111001	1011000110101	265.92	249.97
13	0.5	0.6	2.4371	1.0225	62.0388	40	50	46.1777	56.7909	0111110011110	1111111010100	290.57	266.75
14	0.6544	0.9251	2.6811	1.5854	64.7715	41.2884	50	5.9489	34.9432	1001111010011	1110011011011	215.27	239.19
15	0.5	0.6	1.9389	1.2401	62.6051	40	50	35.1977	2.2806	1101101111111	1010100111111	259.58	215.18
16	0.9552	0.6	1.7695	1.3551	65.9146	40	50	13.3374	33.154	1101100111111	1111111101111	210.96	244.6
17	0.7878	0.6	1.8118	1.6818	72.1854	40	50	90	60	1110111111111	1111111111111	150.62	161.64
18	1.0936	1.178	1.1548	1.6357	120.798	104.9355	77.4118	90	60	1111111111111	1111111111111	88.97	88.97
19	1.082	1.3567	1.4654	1.9428	144.0614	133.447	99.6556	90	60	1111111111111	1111111111111	16.09	16.09
20	0.9036	1.3689	1.4678	1.9869	151.9839	141.929	106.4912	90	60	0001011011101	1001111001101	0	0
21	0.5	1.3294	1.3031	1.9854	105.2404	92.3514	88.0413	90	60	0000100000101	0111111110001	0	0
22	0.913	1.2186	1.3127	1.9395	91.326	71.5959	53.0479	90	60	0100100101111	1111000100111	0	0
23	0.9708	1.3041	1.237	1.8057	89.8788	73.8801	50	90	60	1000100010000	0000110001101	0	0
24	0.5576	1.1561	1.0459	1.9468	83.1988	61.1748	50	90	60	0110111110011	1110100000001	0	0
Fuel cost ($/day)										27218.64			
Emission (lb/day)										3000.24			
Solar cost ($/day)										1361.91			
Wind cost ($/day)										3201.43			

Table 12 Comparison of emission for EES of wind–solar-based HTS system

Algorithms	Emission (lb/day)			Computational time (s)
	Best	Average	Worst	
OWOA	3000.24	3031.87	3923.45	22.3
WOA	3009.98	3053.43	4007.67	38.79
GWO	3221.66	3196.88	4233.54	43.64
SCA Dasgupta et al. (2022)	5290.41	–	–	27.11
BSA Dasgupta et al. (2022)	5747.92	–	–	32.24

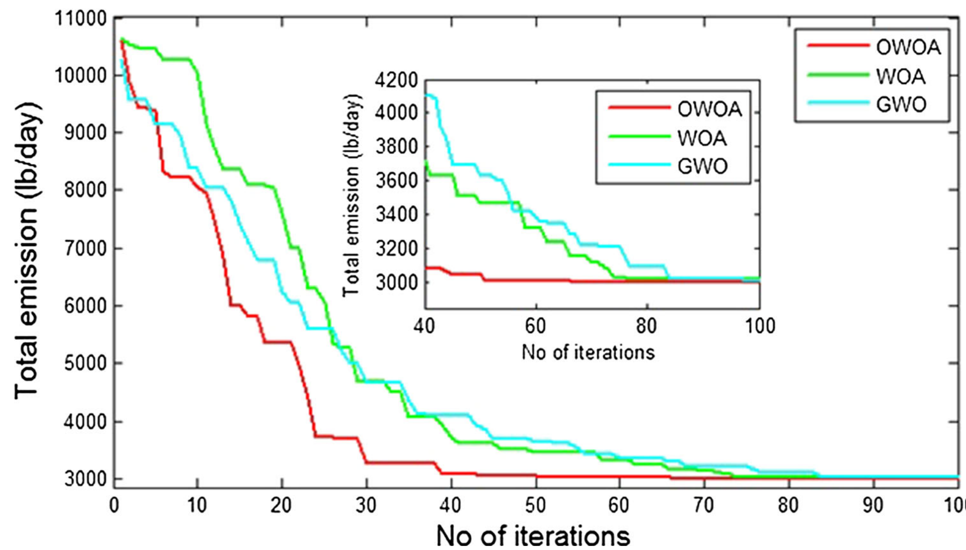

Fig. 12 Emission convergence graph of wind- and solar-based HTS system using different algorithms

(b) Equation (14) represents the operating limits of the hydro generators.

$$P_{Hj,\min} \le P_{Hj}^{t} \le P_{Hj,\max}$$
$$j = 1, 2, ..., N_H;\ t = 1, 2, ..., T_l. \quad (14)$$

In the above mathematical expression, the least and the highest generation of power for the jth hydro generator is represented by $P_{Hj,\min}$and $P_{Hj,\max}$, respectively.

(c) The wind power generation depends on wind speed (m/s). Due to uncertainty of wind speed, the wind power generation will be different. Equation (15) represents the operating limits of the wind generators

$$0 \le P_{wn}^{t} \le P_{wn,\max} \quad j{=}1,2,...,N_w;\ t{=}1,2,...,T_l, \quad (15)$$

where $P_{wn,\max}$ denotes the maximum power generation of the nth wind unit.

(d) The solar power generation depends on the solar radiation and temperature of solar as given in (5). The operating limit of the solar power generation may be formulated as in (16).

$$0 \le P_{sk}^{t} \le P_{sk,\max}^{t} \quad (16)$$

Here, $P_{sk,\max}^{t}$ represents maximum power generation of the kth solar unit.

2.2.2.2 Ramp rate constraint The adjustment of the power outputs is unbounded, which is an unpractical assumption that has prevailed in many past studies for the purpose of simplifying the problem. In practice, however, the ramp rate restriction limits the operating range of all online equipment for changing generator operation between the two operational periods. With appropriate upper and downward ramp rate restrictions, the generation may grow or decrease. As a result of the ramp rate limitations listed below, units are constrained.

If power generation of the tth hour is increased from its previous hour generation, the constraint listed in (17) should be satisfied.

$$P_i{}^{t} - P_i^{t-1} \le ur_i. \quad (17)$$

If power generation of the tth hour is decreased from its previous hour generation, the constraint depicted in (18) should be satisfied;

$$P_i^{t-1} - P_i{}^{t} \le dr_i, \quad (18)$$

Table 13 Optimal results obtained by OWOA for CEES with wind–solar-based HTS system

Hour	Discharge of hydro reservoir ($m^3 \times 10^5$)				Thermal power (MW)			Wind power (MW)		Solar panel on/off status of Plant 1	Solar panel on/off status of Plant 2	Solar power (MW)	
	Q_{h1}	Q_{h2}	Q_{h3}	Q_{h4}	P_{Th1}	P_{Th2}	P_{Th3}	P_{w1}	P_{w2}			P_{s1}	P_{s2}
1	0.8623	0.613	2.0915	1.2435	115.1843	115.4749	140.903	0.0318	28.485	0001001011101	1011001011101	0	0
2	0.7965	0.8702	1.9324	0.8403	103.2501	209.2955	125.5247	16.4581	9.8804	0000101000110	0010101100010	0	0
3	0.8136	0.6282	1.054	1.7064	102.317	124.599	50	19.7665	28.0405	0111101011100	0011011000101	0	0
4	0.7117	0.8791	1.2667	0.7099	103.1315	100.5465	121.1475	21.6991	11.6061	0001100110111	0010110110101	0	0
5	0.6228	1.0664	1.6495	1.2765	102.5964	111.4171	50	5.824	41.778	1010011010010	1111011111011	1.04	1.97
6	0.847	0.7782	2.6997	0.8125	168.9018	212.9396	50	4.9388	13.8637	1111101111111	1111111111111	40.29	43.77
7	0.6446	0.7077	1.0732	0.9448	102.8113	193.1195	139.1622	0	11.8043	1111110111111	1111111100111	100.69	89.51
8	0.7284	0.9191	1.3241	1.1406	102.6653	124.7354	50	14.4648	16.1583	1111110111110	1011101101110	191.61	157.49
9	1.0614	0.7241	1.0023	1.1747	102.3586	97.7626	192.7087	0	14.4534	1101101101101	1111110011011	152.76	165.48
10	1.2732	1.0432	1.6467	1.7536	102.4854	59.8323	125.5	11.884	1.9341	0101101111010	0000010010111	197.85	137.79
11	0.7039	0.7407	1.6928	0.6576	40.2245	57.7824	57.8301	12.4778	13.2716	0111111010111	1101011100110	348.19	271.39
12	1.2474	0.8199	2.6345	1.2611	102.6848	124.1078	50	0	16.5671	1110110101101	0000101110100	313.79	196.78
13	0.5092	0.6912	1.6732	1.6312	23.4617	81.4112	132.3107	7.6212	20.0136	1101100011011	1010101101001	252.46	219.12
14	0.5282	0.8479	2.0162	0.9699	102.3453	50.5919	69.7714	4.5085	14.7055	1011111110110	0110010010111	267.1	195.34
15	0.6915	0.7393	2.899	1.8879	101.6211	123.5485	72.4971	9.2829	0	0001110110011	0101101011010	174.19	163.94
16	1.0254	0.6765	2.1988	1.6601	101.0403	40	137.7841	10.9206	8.4749	1101111001101	0101011111001	180.39	174.27
17	1.1633	0.7842	1.698	1.923	102.9528	115.4713	158.0812	8.0837	35.8291	1101010101011	1001000011011	99.19	77.15
18	0.6729	0.9063	1.7815	1.9621	117.3624	125.0015	240.0149	12.7894	30.7476	0111101111111	1111111111111	77.84	88.97
19	0.7105	0.634	1.6726	1.575	173.0649	209.7058	207.8979	11.2847	29.8192	1111111111111	1111111110111	16.09	14.63
20	0.7699	1.4342	1.2716	1.4793	168.7849	209.0631	136.9772	80.0946	7.4103	0011001010010	0011101101000	0	0
21	0.6081	0.8285	1.5154	1.7482	170.5943	112.7225	104.5427	74.7688	8.6394	0100001010011	0000010110111	0	0
22	0.9608	0.6505	1.8252	1.8492	102.7453	124.8735	138.9543	23.5526	15.7768	1100000111110	1110011110111	0	0
23	0.7042	1.2372	1.4468	1.7553	102.5106	119.0902	131.8119	13.0687	17.6489	1011111101101	1110110011001	0	0
24	0.8432	0.9804	1.4488	1.9956	101.9727	67.4033	137.9862	10.5352	7.9709	0011100000000	1111011000101	0	0
Fuel cost ($/day)										32946.64			
Emission (lb/day)										8096.87			
Solar cost ($/day)										1147.53			
Wind cost ($/day)										5688.44			

Table 14 Comparison of generation cost and emission for CEES of wind–solar-based HTS system

Algorithms	Fuel cost ($/day)	Emission (lb/day)	Computational time (s)
OWOA	32,946.64	8096.87	29.23
WOA	32,960.28	8108.54	50.56
GWO	33,102.76	8132.92	77.36
SCADasgupta et al. (2022)	41,500.00	8061.50	29.28
BSA Dasgupta et al. (2022)	41,995.00	9011.00	39.23

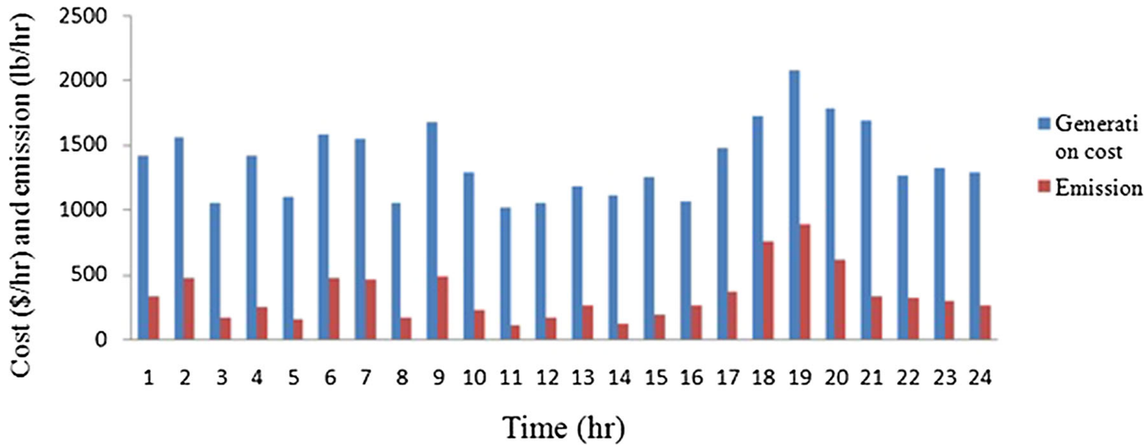

Fig. 13 Cost and emission of thermal units for CEES of HTWSS

where P_i^{t-1}, P_i^t are the power generation of the i^th unit at $(t-1)$th hour and tth hour, respectively, and ur_i and dr_i are the upper and the lower ramp rate limits, respectively.

The addition of ramp rate limitations alters the generator's operation constraints as in (19):

$$\max(P_i^{\min}, P_i^{t-1} - dr_i) \le P_i{}^t \le \min(P_i^{\max}, P_i^{t-1} + ur_i). \tag{19}$$

2.2.2.3 Volumes and discharges limitation of reservoir (a) The maximum and minimum volume of reservoir of hydropower generating is given by (20).

$$v_{Hj,\min} \le v_{Hj}^t \le v_{Hj,\max}$$
$$j = 1, 2, ..., N_H; \; t = 1, 2, ..., T_l \tag{20}$$

In the above-mentioned equation, $v_{Hj,\min}$ and $v_{Hj,\max}$ denote, respectively, the least and the highest storage volume of the jth reservoir.

(b) The maximum and minimum discharge of reservoir of hydropower generating is represented as in (21).

$$q_{Hj,\min} \le q_{Hj}^t \le q_{Hj,\max}$$
$$j = 1, 2, ..., N_H; \; t = 1, 2, ..., T_l \tag{21}$$

In the above equation, the least and the highest discharge rate is defined, in order, by $q_{Hj,\min}$ and $q_{Hj,\max}$ for the jth hydro reservoir.

3 Whale optimization algorithm

Mirjalili and Lewis (2016) introduced WOA which is a meta-heuristic technique and is based on population. WOA is based on hunting activities of humpback whales. Hunting nature of the whales is a unique technique where the whales search for prey in a group or make encircle surrounding the prey.

3.1 Encircling prey

In encircling prey, humpback whales encircle location of the prey. They try to obtain the present finest candidate solution. The fittest solution is considered as the target prey. The other agents change their position and adjust to find a new position which tends towards the finest candidate solution. This concept can be represented by (22):

$$c(\delta + 1) = \vec{Y}^1(\delta) - \vec{E}.\vec{H}$$
$$\vec{H} = \left|\vec{G} \cdot \vec{Y}^1(\delta) - \vec{Y}(\delta)\right|. \tag{22}$$

Table 15 Optimal results obtained by OWOA for ELS of wind–solar-based HTS system with ramp rate function

Hour	Discharge of hydro reservoir ($m^3 \times 10^5$)				Thermal power (MW)			Wind Power (MW)		Solar panel on/off status of Plant 1	Solar panel on/off status of Plant 2	Solar Power (MW)	
	Q_{h1}	Q_{h2}	Q_{h3}	Q_{h4}	P_{Th1}	P_{Th2}	P_{Th3}	P_{w1}	P_{w2}			P_{s1}	P_{s2}
1	1.2922	0.7099	2.2970	0.6416	176.5147	124.9079	139.7598	4.5821	6.4838	0000000111110	1000111001011	0	0
2	0.6499	0.8525	1.0064	1.1522	110.6683	124.9079	139.7528	22.3421	29.2182	0010111010111	1000010111101	0	0
3	0.9355	0.6000	2.0095	0.6000	106.9692	124.8929	139.7598	22.3823	29.2096	1011010010111	0010111101001	0	0
4	0.7695	0.8133	1.6932	1.8609	102.6726	105.0013	50.0001	6.7654	3.7583	0010011100000	0100101010011	0	0
5	0.5529	0.6000	1.8395	1.1069	167.6038	124.9079	50.0000	5.3785	7.3858	1111111111111	1111111111111	2.3404	2.3404
6	0.8704	0.6000	1.8925	1.8396	135.7619	124.9109	50.0000	14.0730	18.2614	1111111111111	1111111111111	43.7734	43.7734
7	0.5452	0.7887	1.1020	1.5820	102.6754	124.5554	138.3399	14.4129	16.1163	1011111111111	1011111111101	103.1798	93.2348
8	0.8403	0.7989	1.3034	1.8228	102.6746	124.9898	50.0000	18.9076	0	1011111001011	0110011101111	154.8644	167.9885
9	0.5000	0.6000	1.1006	0.8349	102.6768	117.5817	139.7537	11.3696	9.5623	1111111111101	1111111111111	203.6736	224.0410
10	0.9130	0.7036	1.5090	1.4404	102.6753	40.0000	112.7891	12.2028	15.0070	0011010110111	1110101111010	204.9153	208.4483
11	0.5598	0.8782	2.1835	0.9195	20.0985	40.0000	50.0000	4.4764	7.8706	1110111110111	1110101111100	378.9170	302.1095
12	0.6641	0.7104	2.0195	1.0461	102.6759	67.2916	123.2715	0.0589	1.5849	0011010111110	1110110010100	308.4707	228.6938
13	0.9830	0.8632	1.4862	1.3806	102.6576	40.0000	50.0000	4.6864	0.0420	1101100001111	0011101110101	252.4628	266.7532
14	0.5000	0.8772	2.4401	1.0607	26.0126	40.0000	50.0000	12.5009	15.3894	0111111110011	1111111111011	271.0847	318.9232
15	1.4034	0.8583	1.0110	0.6980	102.6740	122.8580	50.0000	0	4.7270	0111111000001	1111111100110	150.2816	218.5914
16	0.6496	0.7616	1.4272	1.3202	102.6662	119.9151	138.2932	0	2.7130	1011100011110	1011010100011	162.0448	140.6427
17	0.6132	0.7050	1.8524	1.8940	102.6761	113.7636	101.3234	17.9661	25.1691	0111010111111	0111111111011	130.4133	139.5974
18	0.6568	0.8257	2.5419	1.7754	185.3466	209.8158	139.7598	14.7087	7.8197	1111111111111	1111111111111	88.9654	88.9654
19	0.9843	0.9740	1.7677	1.0524	185.3462	124.9090	229.4598	63.7403	42.7773	1111111111111	1111111111111	16.0930	16.0930
20	1.2738	1.0571	1.9503	1.8830	185.3582	209.8158	139.7531	19.9532	33.8619	1100010001010	0000001000100	0	0
21	1.1325	1.0515	1.8028	1.8158	171.0353	124.8992	139.7598	5.1349	6.9654	1110010000111	1111010110111	0	0
22	0.6168	1.3005	1.5535	1.6079	102.6755	124.9043	139.7556	20.4646	28.6447	1100011001110	0010101001000	0	0
23	0.8325	0.7769	1.3768	1.7870	102.6841	124.9079	138.0464	13.2005	17.4768	1101011100100	1101010111100	0	0
24	0.7612	1.4935	1.5993	1.9911	102.6662	63.6569	112.0068	17.3835	21.9726	1100111111101	1100101111000	0	0
Fuel cost ($/day)										30,454.53			
Emission (lb/day)										7409.9			
Solar cost ($/day)										1278			
Wind cost ($/day)										4680.20			

Table 16 Statistical analysis for ELS results for wind–solar-based HTS system with ramp rate function

Algorithms	Fuel cost ($/day)			Computational time (s)
	Best	Average	Worst	
OWOA	30,454.53	30,481.46	30,523.53	21.3
WOA	30,475.77	30,545.11	30,612.42	34.9

In the above equation, $\vec{E}$, $\vec{G}$ are coefficients, δ denotes current iteration, and the position vector is represented by Y, while Y^1 signifies position vector of the finest solution.

The $\vec{E}$ and $\vec{G}$ are calculated as follows.

$$\vec{E} = 2 \cdot \vec{b} \cdot \vec{l_1} - \vec{b} \tag{23}$$

$$\vec{G} = 2 \cdot \vec{l_2}. \tag{24}$$

In (23)–(24), l_1 and l_2 are random values within [0, 1], while b gradually reduces from 2 to 0.

3.2 Bubble net hunting method

In bubble net searching mechanism, the preys are attacked by the humpback whales. For hunting mechanism, the following mentioned two techniques may be noted.

3.2.1 Shrinking encircling method

In this method, a particular bubble is made beside a circle by the whales when they are swimming nearly close to the prey. The mechanism behaviour ($\vec{b}$) of prey is represented by (25)

$$\vec{b} = 2 - \delta \frac{2}{\text{Maxiter}}, \tag{25}$$

where Maxiter presents the maximum number of iteration.

The search agent updates its position from the original position for hunting the prey. This searching process moves towards the fittest candidate.

3.2.2 Updating position by spiral movement

For hunting the prey, some distance is to be covered by the whales by updating the position. As the movement of humpback whales is helix shaped, the spiral equation, represented in (26), may measure the aforesaid distance:

$$\vec{Y}(\delta + 1) = \vec{H_1} \cdot e^{cT} \cos(2\pi\delta) + \vec{Y^1}(\delta). \tag{26}$$

In above mathematical relation, $\vec{H_1} = \left|\vec{Y^1}(\delta) - Y(\delta)\right|$ signifies distance covered by the ith whale towards the best solution, while the constant of helix shape movement is characterized by c. The range of δ is arbitrary varying within [− 1, 1].

For hunting the prey, whales make a target to swim surrounding them and attack using two mechanisms. The mathematical model of these mechanisms to represent the modified position of whales is given by (27) where the probability of choosing the mechanisms is 50%.

$$\begin{cases} \vec{Y}(\delta + 1) = \vec{Y^1}(\delta) - \vec{E}.H \quad for\, q < \dfrac{1}{2} \\ \qquad = \vec{H_1} \cdot e^{c\delta} \cos(2\pi\delta) + \vec{Y^1}(\delta) \quad \text{for}\, q \geq \dfrac{1}{2} \end{cases}. \tag{27}$$

In above equation, q is arbitrarily varying within [0, 1] during the optimization process.

3.3 Looking for prey

Humpback whale arbitrarily searches the prey. The position of the whale is changed depending upon the location of the other whales. The numerical expression to shift the position of the whale from the original position is as follows:

$$\begin{cases} \vec{H} = \left|\vec{G} \cdot \vec{Y_{\text{rand}}} - \vec{Y}\right| \\ \vec{Y}(\delta + 1) = \vec{Y_{\text{rand}}} - \vec{E}\,\vec{H}, \end{cases} \tag{28}$$

where Y_{rand} is chosen as an arbitrary number varying randomly for a different positions.

4 Opposition-based learning

OBL is a novel approach to improve the search ability and is used to improve solution accuracy of various optimization problems. In order to get best solution, the OWOA searches for the solution in the opposite direction of specified values which is most likely to be nearer to a random number. OBL is planted on opposition-based initialization and opposition-based generation jumping. Mathematically, let $[a, b]$ be a real number, and its opposite number x^0 is represented by (29):

$$x^0 = a + b - x. \tag{29}$$

For n-dimensional, opposite number is represented by (30):

$$x_i^0 = a_i + b_i - x_i. \tag{30}$$

Table 17 Optimal results obtained by OWOA for EES of wind–solar-based HTS system with ramp rate function

Hour	Discharge of hydro reservoir ($m^3 \times 10^5$)				Thermal power (MW)			Wind power (MW)		Solar panel on/off status of Plant 1	Solar panel on/off status of Plant 2	Solar power (MW)	
	Q_{h1}	Q_{h2}	Q_{h3}	Q_{h4}	P_{Th1}	P_{Th2}	P_{Th3}	P_{w1}	P_{w2}			P_{s1}	P_{s2}
1	0.5141	0.6347	1.0644	1.4087	231.9643	50.2502	50.0000	16.8533	42.8239	1001110000110	1000100001111	0	0
2	1.2456	1.0997	2.2985	1.1904	214.7770	62.7567	50.0000	43.5956	49.8718	0100110011110	0110011101011	0	0
3	1.2110	0.8115	2.2552	0.6045	201.3986	81.0011	50.0000	65.2073	28.9405	0010000001011	0100010000110	0	0
4	0.7475	0.6000	2.4460	1.7361	183.9362	43.8894	50.0000	46.8164	18.2578	0011010111010	0000101101000	0	0
5	0.6436	0.7957	1.4086	1.0009	181.9608	44.0206	50.0000	57.2215	29.2693	0111111011111	1011110001101	2.0212	1.3829
6	0.7644	0.8668	1.8370	0.7124	194.2445	98.2732	50.0000	40.7534	41.4710	1111111111111	0111111111111	43.7734	41.7837
7	0.5546	0.7965	1.6549	1.4250	240.3159	51.4860	50.0000	42.3755	12.7245	1110011111111	1111111111111	94.4779	109.3954
8	0.5430	0.6895	1.1197	1.2522	154.9839	40.0000	50.0000	16.8533	50.7574	0111111001110	0001111111111	157.4892	194.2367
9	0.5784	0.6000	1.8811	1.4116	164.7278	45.0459	50.0000	27.5032	31.2110	1111111111111	1111111101111	224.0410	203.6736
10	0.6999	0.6000	2.4264	1.8727	180.5850	40.0000	50.0000	0	10.8982	1111011010111	1101101101011	233.1795	211.9813
11	0.8691	0.6000	1.4317	1.1144	106.6180	40.0000	50.0000	29.1107	37.8933	0001111010110	0100010010111	256.0250	225.3020
12	0.5411	0.6000	2.2083	1.5684	130.5155	40.0000	50.0000	8.2981	18.3354	1110010011101	1010110100111	281.8784	287.1968
13	0.5959	0.6000	1.9924	1.2521	105.4093	40.0000	50.0000	41.8257	29.0987	1111011010110	0100111010101	276.2801	233.4090
14	0.5335	0.6000	1.5324	0.7462	168.7477	40.0000	50.0000	36.4706	18.1417	1010110011100	1111110101100	183.3808	227.2328
15	0.6256	0.6000	2.3370	0.7029	94.2637	46.2543	50.0000	1.7089	34.1285	1111111110110	1011110111111	245.9153	259.5772
16	0.8064	0.6000	1.4256	1.3095	122.2939	45.8310	50.0000	7.3251	27.4797	1111111111101	1110110001011	244.5960	155.9299
17	0.5908	0.6275	1.6639	1.5136	135.0154	40.0000	50.0000	69.2228	30.8028	0111111111111	1111111111111	154.2918	161.6391
18	1.1731	0.9465	1.8142	1.8269	248.9357	96.8771	72.2795	27.5032	19.3254	1111111111111	1111111111111	88.9654	88.9654
19	1.0020	1.3688	1.2140	1.9470	263.3751	124.8595	57.7164	52.0766	34.7730	1111111111111	1101111111111	16.0930	15.1786
20	1.2861	1.3327	1.0075	1.8338	302.4354	126.5457	72.9831	26.9418	18.3354	0010010110101	1100001011000	0	0
21	1.2275	1.0237	1.1708	1.7862	215.5349	83.0151	56.5960	27.5032	33.2658	1101110001010	0010011011010	0	0
22	1.0989	1.1408	1.7021	1.8970	191.9549	50.4128	50.0000	27.3867	42.4743	1010010101001	0100001011010	0	0
23	0.8653	1.2221	1.1852	1.8246	200.4186	46.1468	50.0000	45.0350	24.6594	1000111110011	1000000100111	0	0
24	0.7826	1.4435	1.3988	1.7617	172.2405	40.0000	50.0000	42.7372	24.1115	0110011111010	1010001100001	0	0
Fuel cost ($/day)										30588.43			
Emission (lb/day)										7235.11			
Solar cost ($/day)										1277.37			
Wind cost ($/day)										12738.0			

Table 18 Statistical analysis for EES results for wind–solar-based HTS system with ramp rate function

Algorithms	Emission (lb/day)			Computational time (s)
	Best	Average	Worst	
OWOA	7235.10	7242.72	7293.42	22.48
WOA	7237.76	7249.19	7312.25	39.12

4.1 OWOA algorithm

The following steps are adopted to solve OWOA algorithm.

Step 1: Initialize the solutions according to population size.
Step 2: Initialize the control variables randomly within maximum and minimum limit in such a manner that all equality and inequality constraints are satisfied.
Step 3: Create opposite population by using (29) and (30) and the control variables of every population set are updated and feasibility of each solution is verified.
Step 4: Calculate the fitness value of population as well as opposite population set.
Step 5: Choose N_p numbers of fittest solution from the population and the oppositional population sets.
Step 6: Fittest values are shorted in the form of finest to worst.
Step 7: Some solutions are kept as elite solutions.
Step 8: The independent variables of non-elite solutions are updated using three approaches, namely 'encircling prey', 'bubble net hunting' and 'search for prey' and if any independent variable violates its operating limit, fix the value to its limiting value.
Step 9: Dependent variables are updated using the equality constraint and verify feasibility of each solution set. Infeasible solution are replaced by feasible solution.
Step 10: Using jumping rate, the opposite population is generated from new population while following (31).

$$\left\{\begin{array}{l}\text{if rand }(0,\ 1) < J_R\ (J_R = \text{jumping rate})\\ \quad \text{for } i = 1:\ N\ (N = \text{Population size})\\ \quad\quad \text{for } k = 1:\ N_c\ (N_c = \text{No of control var}\,iables)\\ \quad\quad\quad \overset{0}{X}_{ik} = a_k + b_k - X_{ik}\\ \quad\quad \text{end}\\ \quad \text{end}\\ \text{end}\end{array}\right. \tag{31}$$

Step 11: The fitness values of opposite population are to be calculated.
Step 12: Np numbers of fittest values are taken from current population and opposite population.
Step 13: Repeat from Step 6 for next iteration.

The flow chart along with mathematical modelling of the proposed OWOA approach is illustrated in Fig. 2.

4.2 OWOA algorithm applied to renewable energy-based HTS problem

The following steps are followed to solve the chosen problem while employing the proposed OWOA algorithm.

Step 1: Input parameters, population size, maximum iteration for the specific problem are initialized. In addition, the constraints of the problem are defined.
Step 2: The rate of discharge of water of hydro generator for each hydro unit up to $(t-1)$ hours is randomly initialized between their operating limits, and discharge rate of water for the final period for total number of hydro units is calculated by using (12) which must be within limiting range. Otherwise, the set of the result is entirely redundant. This process is continued, until or unless no violation of discharge velocity takes place.
Step 3: Furthermore, the volume of each reservoir for every hour is analysed by applying (11) and they must satisfy the inequality constraints stated in (20). Otherwise, the set of solution is needed to be eliminated and re-initialize the solution set.
Step 4: Afterwards, calculate the hydropower generation of each unit for 24 h using (10), if generating power for any unit is less than zero, then it is made equal to zero.
Step 5: The generation of hydro units using (10) helps to calculate the generation of thermal, wind and solar while satisfying power balance equations stated in (8). This generation must satisfy the inequality constraints.
Step 6: The each hour generation of the first thermal unit is initialized randomly for 24 h among the total generation by thermal, wind and solar generators. Afterwards, the thermal generations of the slack unit for all the intervals are calculated, which must be within the limiting range. If an infeasible solution is reached, that result is replaced by generating a new feasible solution.
Step 7: Fitness value for an individual member of the population set is calculated.

Table 19 Optimal results obtained by OWOA for CEES of wind–solar-based HTS system with ramp rate function

Hour	Discharge of hydro reservoir ($m^3 \times 10^5$)				Thermal power (MW)			Wind power (MW)		Solar panel on/off status of Plant 1	Solar panel on/off status of Plant 2	Solar power (MW)	
	Q_{h1}	Q_{h2}	Q_{h3}	Q_{h4}	P_{Th1}	P_{Th2}	P_{Th3}	P_{w1}	P_{w2}			P_{s1}	P_{s2}
1	1.2922	0.7099	2.297	0.6416	176.5281	124.8978	139.7598	4.6557	6.4068	0 0 0 0 0 0 1 1 1 1 1 1 0	1 0 0 0 1 1 1 0 1 1 0 0 1	0	0
2	0.6499	0.8525	1.0064	1.1522	110.8	124.892	139.7528	22.2123	29.2335	0 0 0 1 0 1 1 0 1 1 0 0 0	1 0 1 0 0 1 1 1 1 1 1 0 1	0	0
3	0.9355	0.6	2.0095	0.6	108.597	124.8929	140.0386	20.5019	29.2027	1 1 1 1 0 0 0 0 1 0 1 1 0	0 0 0 0 0 1 0 0 0 1 0 0 1	0	0
4	0.7695	0.8133	1.6932	1.8609	102.6783	104.9957	50.0001	6.7654	3.7583	0 0 1 0 0 0 1 1 0 0 0 0 0	1 1 0 0 1 1 1 0 0 0 0 1 1	0	0
5	0.5529	0.6	1.8395	1.1069	102.6754	112.9409	110.6893	20.2907	10.725	1 0 0 0 0 1 0 0 0 1 1 1 0	0 0 1 0 1 1 1 0 1 0 0 0 1	0.9308	1.0904
6	0.8704	0.6	1.8925	1.8396	102.8534	124.9156	87.7106	21.9061	15.299	1 1 1 0 0 1 1 1 1 1 1 1 1	1 1 1 1 1 1 1 1 1 1 1 1 0	37.8043	39.794
7	0.5452	0.7887	1.102	1.582	102.944	124.5554	141.8094	14.4129	16.1163	1 0 1 1 1 1 1 1 1 1 1 1 1	1 1 1 1 1 1 1 1 0 1 1 0 1	103.1798	89.5054
8	0.8403	0.7989	1.3034	1.8228	102.6109	96.9001	111.0788	19.8614	0	1 0 1 1 1 1 1 0 0 1 0 0 1	0 0 1 0 0 1 1 1 0 1 1 1 1	133.8658	154.8644
9	0.5	0.6	1.1006	0.8349	102.6824	117.5817	139.7537	11.3696	9.5568	1 1 1 1 1 1 1 1 1 1 1 0 1	1 1 1 1 1 1 1 1 1 1 1 1 1	203.6736	224.041
10	0.913	0.7036	1.509	1.4404	102.6163	40	112.7891	12.2028	15.0651	0 0 1 1 0 1 0 1 1 0 1 1 1	1 1 1 0 1 0 1 1 1 1 0 1 0	204.9153	208.4483
11	0.5598	0.8782	2.1835	0.9195	20.0043	40	117.8026	12.7544	7.8706	1 1 1 0 1 1 0 1 0 0 1 1 1	1 1 1 0 1 0 1 1 1 1 1 0 0	302.1095	302.1095
12	0.6641	0.7104	2.0195	1.0461	102.6312	67.2916	123.3156	0.0591	1.5849	0 0 1 1 0 1 0 1 1 1 1 1 0	1 1 1 0 1 1 0 0 1 0 1 0 0	308.4707	228.6938
13	0.983	0.8632	1.4862	1.3807	102.8046	40	50	4.5526	0.0245	1 1 0 1 1 0 0 0 0 1 1 1 1	0 0 1 1 1 0 1 1 1 0 1 0 1	252.4628	266.7532
14	0.5	0.8772	2.4401	1.0607	89.9245	40	50	12.0829	11.6191	0 1 1 1 1 1 0 1 1 0 0 1 1	1 1 1 1 1 1 1 1 1 1 0 0 1	243.1789	287.0309
15	1.4034	0.8583	1.011	0.698	102.6744	122.858	108.3979	0	21.0793	0 1 1 1 1 1 1 0 0 0 0 0 0	1 1 1 1 0 1 1 1 0 0 0 1 0	122.9576	170.7745
16	0.6496	0.7616	1.4272	1.3202	101.7825	119.6724	138.2932	0	3.8254	1 0 1 1 1 0 0 0 1 1 1 1 0	1 0 1 1 0 1 0 1 0 0 0 1 1	162.0448	140.6427
17	0.6132	0.705	1.8524	1.894	102.6761	113.7636	101.3234	17.9661	25.1703	0 1 1 1 0 1 0 1 1 1 1 1 1	0 1 1 1 1 1 1 1 1 1 0 1 1	130.4133	139.5974
18	0.6568	0.8257	2.5419	1.7754	185.3177	209.8739	138.599	16.9679	6.6796	1 1 1 1 1 1 1 1 1 1 1 1 1	1 1 1 1 1 1 1 1 1 1 1 1 1	88.9654	88.9654
19	0.9843	0.9731	1.766	1.0524	185.3373	124.9079	229.4459	63.7403	42.7853	1 1 1 1 1 1 1 1 1 1 1 1 1	1 1 1 1 1 1 1 1 1 1 1 1 1	16.093	16.093
20	1.2987	1.0571	1.9503	1.883	185.2725	209.8237	127.3751	19.4095	46.1661	1 1 0 0 0 1 0 1 0 1 0 0 0	1 0 0 0 0 0 1 0 0 0 1 0 0	0	0
21	1.1325	1.0515	1.8005	1.8158	170.568	125.5985	139.7173	4.831	7.0578	1 1 1 0 0 1 0 0 0 0 1 0 1	1 1 1 1 0 1 0 1 1 0 1 1 1	0	0
22	0.6168	1.3005	1.6482	1.6072	104.4848	124.9043	139.7556	20.2736	29.0406	1 1 0 1 0 1 1 0 0 1 1 1 0	0 0 1 0 1 0 1 0 0 0 1 1 0	0	0
23	0.8325	0.7713	1.1943	1.787	102.6779	125.1745	138.0464	13.3682	17.4768	1 1 1 1 0 1 1 1 0 0 1 0 0	1 0 0 1 1 1 0 1 1 1 1 0 0	0	0
24	0.7364	1.5	1.7151	1.9899	102.8176	63.6569	112.0068	17.3835	25.9655	1 0 0 0 1 0 1 1 1 1 1 0 1	1 1 0 0 1 0 1 1 1 1 0 0 0	0	0
Fuel cost ($/day)										31908.73			
Emission (lb/day)										7576.15			
Solar cost ($/day)										1207.81			
Wind cost ($/day)										5138.31			

Table 20 Comparison of generation cost and emission for CEES of wind–solar-based HTS system with ramp rate function

Algorithms	Fuel Cost ($/day)	Emission (lb/day)	Computational time (s)
OWOA	31908.73	7576.15	31.12
WOA	31912.73	7582.36	52.23

Step 8: After calculation of oppositional population set, calculate the fitness value of oppositional population.

Step 9: Make an initial population set with N_p numbers of fittest values from the current population and opposite population.

Step 10: The encircling prey, bubble net hunting technique, search for prey (exploration phase) steps of OWOA algorithm are applied to non-elite solutions to modify the independent variables. In OWOA method, the obtained initial finest result is considered as the objective prey. To get the best position, the other search agents attempt to improve their location in the direction of finest search agent using the approaches described above. The new status of every agent signifies the discharge rate of water for each hydro plants for $(t-1)$ hours, the wind generation units and the generation of thermal power for (N_s-1) number of thermal generators during each time period.

Step 11: Based on a jumping rate value, opposite population is generated and fitness value of the opposite population is calculated.

Step 12: After getting current and opposite population, all the values are sorted and rearranged in ascending order.

Step 13: Few solutions are kept as best solutions.

Step 14: Check whether the updated values of the specific problem are within operating limits or not. The independent variable is considered as the least value, if it is less with respect to the minimum value and makes it equivalent to the highest value, if it is more than the most significant value.

Step 15: Check the feasibility of the slack units. If it is not satisfied, the solution is replaced by the currently generated best feasible solution. A newly developed results follow duplicate solutions.

Step 16: Final optimal solution will be reached.

5 Simulation results and discussion

5.1 Case study 1: benchmark functions

The benchmark is a tool by which the strength or weakness of optimization technique can be determined. The effectiveness of the proposed OWOA has been investigated by choosing a group of 29 benchmark functions. The population size and iteration cycle for OWOA and WOA are considered as 50 and 500, respectively. The individual benchmark function is run for 50 times. The total benchmark functions are classified into four different groups firstly unimodal functions $(F_1(x)$ to $F_7(x))$ to judge exploitation of the optimization technique. Detailed description of the unimodal benchmark functions is discussed in Table 21 of Appendix Section. Results of Table 1 represent better performances of the proposed OWOA algorithm. Secondly, multimodal functions $F_8(x)$ to $F_{13}(x)$ are discussed detailed in Table 22 of Appendix Section to evaluate the searching capability of an optimization technique. Results presented in Table 1 show the searching superiority of the proposed OWOA algorithm. Thirdly, the fixed-dimensional multimodal benchmark functions $(F_{14}(x)$ to $F_{23}(x))$ are prescribed in Table 23 of Appendix Section. Using these functions, the obtained results show better exploration of OWOA optimization technique. Finally, various composite functions, described in Table 24 of Appendix Section, are considered and the simulation results of various algorithms for these functions are listed in Table 2. The success of the proposed OWOA algorithm for composite functions shows about the avoidance of local optimality. The convergence graphs of various benchmark functions for OWOA and WOA algorithms, illustrated in Figs. 3-6, show the superiority of OWOA over the basic WOA.

5.2 Case study 2: HTS and HTWSS

Two test systems with transmission losses are preferred in this presentation to illustrate the performance of the recommended OWOA technique. In the first test method, three thermal and four hydro units have been considered. Thereafter, two wind power units and two solar units are incorporated with the first test system for making a second test system. Power generation limit, cost and emission coefficients for thermal units are presented in Table 25 of Appendix Section. The performance of these two test systems has been checked for 24 h for the individual hour interval. The water time delay, as in Table 26 of Appendix Section, is considered in the hydro system when water falls from one reservoir to another reservoir. Inflow in the reservoir for 24 h and reservoir capacity, discharge, generation limit with initial and final condition are provided in Tables 27 and 28 of Appendix Section.. The different coefficient values for hydropower generation, as formulated in (10), are presented in Table 29 of Appendix section. The B loss coefficients are generated from reference Basu (2006) and illustrated in Table 30 in Appendix Section. In second test system, the wind and solar power units are incorporated with HTS system. The cut in speed, cut out seed, rated speed and coefficients of wind generation are discussed in detail in Table 31 of Appendix Section.. The variation of solar radiation and temperature for 24 h is provided in Table 32 of Appendix Section. The dynamic load demand for 24 h of the system is elaborated in Table 32 of Appendix Section. The solar power generations for solar panel with unit rate are illustrated in Table 33 of Appendix Section. Power generation limit and ramp rate limit for thermal units are displayed in Table 34 of Appendix Section. The transmission loss coefficients of the proposed system are illustrated in Table 35 of Appendix Section. The MATLAB programming is done with the help of a personal computer with a core i5 processor, 500 GB, 4 GB RAM. The population size is considered as 50. To get the best results, the programming is run for 100 numbers of iterations, for each test system.

5.2.1 Test system-1

For test system-1, three thermal generators in addition to four hydro units are taken for exhibiting the achievement of the presented technique. In this problem, the transmission loss is additionally considered. The total load demand of the proposed system is considered 22650 MW. The primary aim as regards the above technique is to diminish the fuel cost and the emission of thermal units. At first, the economic load scheduling (ELS) is considered which provides generation of active power by various units for 24 intervals in a day. For ELS, MATLAB programming has been run for 50 different populations using OWOA, WOA and GWO. The most favourable water discharge of hydro generators, active power generation of thermal generators for each hour and generation of fuel cost with emission for individual hour are listed in Table 3. The convergence graph of the presented technique (*i.e.* OWOA) is compared with WOA and GWO in Fig. 7. From the characteristic, it has shown that the proposed method is converging at 28 iterations which is much faster than the other techniques. Comparison of generation cost of the proposed algorithm with the other techniques such as WOA, GWO, quantum-inspired evolutionary algorithm (QEA), DE, small population-based PSO (SPSO) and fuzzy-based evolutionary programming (Fuzzy EP) is made in Table 4. The computation time for the proposed method to solve the problem is 18.1 s, and the best cost of fuel is obtained is 43,988 \$/day, whereas the computational time and fuel cost using WOA are 27.8 s and 44002 \$/day, using GWO are 38.6 s and 44182 \$/day, and for QEA, SPSO, DE, Fuzzy EP the obtained costs are 44686 \$/day, 44980 \$/day, 44526 \$/day, 45063 \$/day. From the results of Table 4, it has been proved that the generation cost as well as the computational time is less with respect to the other techniques. The characteristic of reservoir volume for cost minimization is represented in Fig. 8.

Secondly, to judge the performance of the presented WOA and OWOA methods, an attempt for economic emission scheduling (EES) is made. The comparison of the simulation results along with CT for EES obtained by the suggested WOA and OWOA methods with other another method, namely GWO, is reported in Table 6. The water discharge for every hour of hydro reservoirs along with power generation by thermal units for economic emission scheduling (EES) is displayed in Table 5, and the hydropower generation by hydro units for EES is displayed in Fig. 9. The comparison of emission results as well as computation time for EES obtained using different methods is represented in Table 6. The computation time to solve the problem is 19.12 s, and the total emission is 21019.16 lb/day which is better than other optimization techniques mentioned in Table 6. The best, average and worst emission, obtained using OWOA, is 21019.16 lb/day, 21055.39 lb/day and 21787.43 lb/day, respectively. Difference of the best result with average is 36.23 and with worst is 768.27 which are better than WOA and GWO optimization techniques. This proves the robustness of the proposed OWOA optimization technique for emission optimization.

Again, the proposed method (*i.e* OWOA) is applied in combined economic emission scheduling (CEES) to verify the efficiency. The main interest of CEES is to reduce both the fuel cost and the emission simultaneously. The CEES may be considered as a bi-objective function as in this scheduling, both fuel cost and emission are two objective functions. A price penalty factor has been considered for solving this bi-objective function, which alters these objective functions into a single-objective function. During optimization, the value of penalty factor is chosen properly as it brings the emission along with fuel cost in the same priority level. The control variables such as the water discharge rate of hydro generators, active power generation of thermal generators for each hour and generation of fuel cost along with emission of individual hour for CEES are illustrated in Table 7. The generation cost and emission for each hour of CEES are displayed in Fig. 10. The volume of reservoir water is varying accordingly with the input and discharge of water from the reservoir for each hour. Due to the change of water volume, the generation of hydropower is also varied with time. The comparison of fuel cost and emission results along with computation time for CEES acquired by the above techniques with other methods is reported in Table 8. Computation time for the proposed method is 28.34 s, and the best fuel cost is found to be 46794.13 \$/day, whereas the amount of emission is found to be 22559.92 lb/day. It is obvious from the results of ELS, EES, CEES that the fuel cost and emission along with computational time for the proposed method are much less with respect to the other reported results yielded by different methods.

5.2.2 Test system-2 without ramp rate function

In a second test system, two wind power, two solar units are incorporated with first test system to check the efficiency of the renewable resources. The first wind power unit consists of 30 turbines, and second wind power unit consists of 20 turbines. The effect of valve point loading is also considered by adding a sinusoidal function with fuel cost to demonstrate the effectiveness of the suggested algorithm under nonlinear environment. Overestimation and underestimation costs for wind units are shown in (2) and (3), respectively. As the wind cost is significantly less as compared to the thermal cost, the wind energy is operated near its rated value. Eleven generating units (four hydro, three thermal, two winds and two solar) provide the total load demand for individual hour. The unbalanced coefficient of underestimated and overestimated is taken at 2.2 MWh and 4.0 MWh , respectively. The cut in speed (the minimum speed of wind) is near about 3.5 m/s at which the turbine starts to rotate. Rated speed is normally 15 m/s of wind at which the wind turbine generates the maximum power on the running condition. Cut out speed, which is more than the rated speed, is generally 25 m/s. At the cut out speed, the wind turbine stops generating electricity to protect the turbine. Furthermore, each solar unit consists of thirteen solar panel. Solar generation depends on intensity, temperature and irradiance of the sun light. Solar intensity and irradiance are different for different geometrical locations and weather conditions. These may produce uncertain behaviour of solar generation. Due to uncertain behaviour of the wind and solar, the test system became more complex. For the random nature of wind speed and short-term calculation, the wind speed parameters are calculated from statistical analysis of the wind speed data for each interval of time. For MATLAB programming of this problem, 50 different random numbers are selected for various initial populations to validate the presented OWOA-based approach. The control variables of second test system are water discharge rate of hydro units, switching operation of solar panels, active power generation by thermal, wind and solar units. In Table 9, the variation of control variables for each hour of all the generators and fuel cost with emission for ELS is discussed. The hydropower generations of the hydro generators are varying for every hour with change in the reservoir volume. The power generated by all the thermal, hydro, wind and solar for each hour is represented in Fig. 11. In Table 10, the comparison of statistical results of fuel cost and computation time for ELS achieved from the presented OWOA method with WOA, GWO, SCA (Dasgupta et al. 2022) and BSA (Dasgupta et al. 2022) are exhibited. The obtained fuel cost and computational time using the proposed algorithm are 32,059.43 $/day and 20.1 s, respectively, which are less than the other methods. After incorporating wind and solar sources with HTS, the obtained fuel cost using OWOA is found to be 32,059.43 $/day, whereas for HTS without renewable energy sources, the obtained fuel cost is 43988 $/day, meaning the proposed technique reduces the fuel cost after incorporating the nonlinearities like wind and solar energy sources with the HTS system. So, due to better tuning ability of the parameters of the proposed OWOA technique, it may easily deal with higher nonlinearity and provides optimal solution.

Again for solving EES and CEES, 50 various populations with arbitrary numbers are taken into consideration. The most favourable hourly water discharge rate of hydro generators, active power generation by means of thermal and wind generators for each hour and generation cost along with emission for individual hour acquired by the preferred algorithm for EES are listed in Table 11. Comparison of emission of the proposed algorithm with the other techniques such as WOA, GWO, SCA (Dasgupta et al. 2022) and BSA (Dasgupta et al. 2022) is made in Table 12. The best emission obtained by OWOA is 3000.24 lb/day, whereas the emission achieved by using WOA is 3009.98 lb/day, using GWO is 3221.66 lb/day, using SCA (Dasgupta et al. 2022) is 5290.41 lb/day, and using backtracking search algorithm (BSA) (Dasgupta et al. 2022) is 5747.92 lb/day. From the results of Table 12, it has been proved that the emission achieved by OWOA is significantly less with respect to the other discussed techniques. The convergence characteristic for emission of different optimization methods is shown in Fig. 12. The proposed method converges faster with respect to the other methods. The obtained total fuel cost, wind cost, solar cost and emission for 24 h are 27218.64 $/day, 3201.43 $/day, 1361.91 $/day and 3000.24 lb/day, respectively. The comparison result of emission and computational time for different methods is displayed in Table 12.

It is already discussed for the previous test system that, to make the bi-objective function of CEES into a single-objective function, a penalty factor is to be taken into account. The control variables like water discharge rate of hydro generators, active power generation from the thermal, wind along with solar units for each hour and generation of fuel cost with emission for individual hour attained by the suggested algorithm for CEES are listed in Table13. The generation cost and emission for each hour of CEES are displayed in Fig. 13, and the comparative results of fuel cost and emission along with computational time are tabulated in Table 14. It is also noticed that the outcomes obtained by using the OWOA technique are significantly superior than the other techniques considered in the article for solving HTWSS problem and it is also true that the proposed method is much faster than the previous approaches as shown in the simulation results.

5.2.3 Test system-2 with ramp rate function

Thermal units can only adjust their output power by a fixed amount, and hence, ramp rate constraints must be taken into consideration. When the observed ramp rate exceeds the limit, the output power should be reduced from the maximum available value to reduce the change rate and then the ramp rate profile should be followed. It determines how rapidly a plant's output can be changed. It is usually computed as the difference between a unit's minimum and maximum capabilities. In addition of valve point loading, wind–solar uncertainty and another nonlinear function like ramp rate function have been included for dynamic operation of the proposed HTS system. Power generation limit and ramp rate limits for thermal units are illustrated in Table 34 of Appendix Section, whereas cost and emission coefficients for thermal units are presented in Table 25 of Appendix Section. The rest of the system data are same as test system-1

For MATLAB programming of this problem, 50 different random numbers are selected for various initial populations to validate the efficacy of the presented OWOA-based approach. The control variables of second test system are water discharge rate of hydro units, switching operation of solar panels, active power generation by thermal, wind and solar units. In Table 15, the variation of control variables for each hour of all generators and fuel cost with emission for ELS is discussed. In Table 16, the comparison of statistical results of fuel cost and computation time for ELS achieved from the presented method are exhibited. The obtained fuel cost and computational time using proposed algorithm, in order, are 30,454.53 $/day and 21.3 s, which are less than the WOA method.

Again for EES, the variation of control variables for each hour acquired by the preferred algorithm is listed in Table 17. The comparison results of emission and computational time for the proposed methods are displayed in Table 18. The obtained emission using OWOA is 7235.10 lb/day and for WOA is 7237.76 lb/day which is the evidence of optimal solution offered by OWOA optimization technique. The statistical analysis of best, average and worst emission results proves the robustness of OWOA technique in solving emission minimization problem.

In CEES, both cost and emission are minimized simultaneously. The control variables like water discharge rate of hydro generators, active power generation from the thermal, wind along with solar units for each hour and generation of fuel cost with emission for individual hour attained by the suggested algorithm for CEES are listed in Table19. The comparison results of fuel cost and emission along with computational time are tabulated in Table 20. It is also noticed that the outcomes, obtained by using the OWOA technique, are significantly superior than the other techniques considered in the article for solving HTWSS problem and it is also true that the proposed method is much faster than WOA technique as shown through different results.

5.2.4 Outcome of simulation study

The obtained simulation results from the proposed systems establish the superiority of the proposed optimization (*i.e.* OWOA) technique in terms of optimal solution, faster convergence rate, less computational time, better tuning ability of the control parameters and dealing capability with highly nonlinear-based system. The evidence of the aforesaid advantages, *i.e.* (i) excellent convergence profile, (ii) global searching ability (iii) robustness and (iv) computational speed, is illustrated below:

- **Excellent convergence profile:** It is observed from the convergence graphs illustrated in Figs. 7 and 12 that OWOA requires less number of iterations to convergence as compared to other methods. Therefore, it is proved that convergence characteristic of the proposed OWOA method is better than the other discussed method(s).
- **Global searching ability:** The obtained results of Tables 4, 6, 8 for HTS, Tables 10, 12, 14 for HTWSS and Tables 16, 18, 20 for HTS with ramp rate limits are the evidences of optimal solutions using OWOA for both single and multi-objective functions. From the results, it is also observed that, by incorporating wind and solar with HTS system, fuel cost and emission get reduced which is also the evidence of high tuning ability of the parameters and high dealing capability with nonlinear system of OWOA technique.
- **Robustness:** From the statistical results illustrated in Tables 6 and 12, it may be observed that the proposed OWOA algorithm seems to be quite robust compared to the other algorithms as the best, mean and worst values for OWOA are quite close to each other. Thus, statistical results depict the evidences of robustness of the proposed OWOA technique.
- **Computational speed:** From the computational time illustrated in Tables 4, 6, 8, 10, 12, 14, 16, 18 and 20 for different case studies, it is observed that hybridization of oppositional-based learning with WOA effectively reduces the computational time which proves the superiority of the OWOA technique over the other prevailing technique(s) in terms of computational speed.

6 Conclusions

Initially, twenty-nine benchmark functions are considered in order to judge the performance of the proposed OWOA and the studied WOA algorithms in terms of exploration, exploitation, local optimality avoidance and convergence speed. Latter on, an attempt has been made to study the HTS and HTWSS problems of interconnected power system. Initially, generation cost and emission are minimized individually, and finally, they are optimized simultaneously. It is proved from the simulation study that the proposed OWOA method yields quality solutions for the studied problems. It is also clear from the simulation study that the suggested OWOA is much efficient compared to other optimization techniques to solve the HTS problem. In HTWSS problem, two wind and two solar units are integrated with the conventional HTS system for minimizing the fuel cost along with emission. Integrating wind as well as solar units in HTWSS system, generation cost and emission are becoming less compared to traditional HTS system. The effectiveness of renewable energy sources is proven to be a superior choice for the utility. Moreover, OWOA has good convergence nature and can easily converge the quality solution. The limitation of premature convergence can be excluded for this new OWOA approach compared to other methods. Though in the present research work, transmission loss coefficients data are taken from literature, in future, ANN-based technique can be adopted to replace the B loss coefficients data of the transmission lines.

Funding The authors have not disclosed any funding.

Data Availability The authors confirm that the data supporting the findings of this study are available within the article.

Declarations

Conflicts of interest The authors do hereby declare that they do not have any conflict of interest.

Research involving human participants and/or animals This article does not contain any studies with human participants or animals performed by any of the authors.

Informed consent Not applicable.

Appendix

The detailed descriptions of the test benchmark functions are noted in Tables 21, 22, 23 and 24. Different parameters and coefficient of thermal, hydro, wind and solar units with load demand and transmission losses are displayed in Tables 25, 26, 27, 28, 29, 30, 31, 32 and 33.

Table 21 Detailed description of unimodal benchmark functions

Functions	Dimension	Range	f_{min}
$F_1(x) = \sum_{i=1}^{n} x_i^2$	30	[−100, 100]	0
$F_2(x) = \sum_{i=1}^{n} \lvert x_i \rvert + \prod_{i=1}^{n} \lvert x_i \rvert$	30	[−10, 10]	0
$F_3(x) = \sum_{i=1}^{n} \left(\sum_{j=1}^{i} x_j \right)^2$	30	[−100, 100]	0
$F_4(x) = \max \{ \lvert x_i \rvert \} \quad 1 \le i \le n$	30	[−100, 100]	0
$F_5(x) = \sum_{i=1}^{n-1} 100(x_{i+1} - x_i^2)^2 + (x_i - 1)^2$	30	[−30, 30]	0
$F_6(x) = \sum_{i=1}^{n} (x_i + 0.5)^2$	30	[−100, 100]	0
$F_7(x) = \sum_{i=1}^{n} i x_i^4 + random\,(0, 1)$	30	[−1.28, 1.28]	0

Table 22 Detailed description of multimodal benchmark functions

Function Name	Dimension	Range	f_{min}
$F_8(x) = \sum_{i=1}^{n} -x_i \sin\left(\sqrt{\lvert x_i \rvert}\right)$	30	[−500, 500]	−418.9829
$F_9(x) = \sum_{i=1}^{n} \left(x_i^2 - 10\cos(2\pi x_i) + 10\right)$	30	[−5.12, 5.12]	0
$F_{10}(x) = -20\exp\left(-0.2\sqrt{\frac{1}{n}\sum_{i=1}^{n} x_i^2}\right) - \exp\left(\frac{1}{n}\sum_{i=1}^{n}\cos(2\pi x_i)\right) + 20 + e$	30	[−32, 32]	0
$F_{11}(x) = \frac{1}{4000}\sum_{i=1}^{n} x_i^2 - \prod_{i=1}^{n}\cos\left(\frac{x_i}{\sqrt{i}}\right) + 1$	30	[−600, 600]	0
$F_{12}(x) = \frac{\pi}{n}\left\{10\sin(\pi y_1) + \sum_{i=1}^{n-1}(y_i - 1)^2\left[1 + 10\sin^2(\pi y_{i+1})\right] + (y_n - 1)^2\right\} + \sum_{i=1}^{n} u(x_i, 10, 100, 4)$	30	[−50, 50]	0
$y_i = 1 + \frac{x_i + 1}{4}$			
$F_{13}(x) = 0.1\left\{\sin^2(3\pi x_1) + \sum_{i=1}^{n}(x_i - 1)^2\left[1 + \sin^2(3\pi x_i + 1)\right] + (x_n - 1)^2\left[1 + \sin^2(2\pi x_n)\right]\right\}$			
$+ \sum_{i=1}^{n} u(x_i, 5, 100, 4)$	30	[−50, 50]	0

Table 23 Detailed description of fixed-dimensional multimodal benchmark functions

Functions	Dimension	Range	f_{min}
$F_{14}(x) = \left(\frac{1}{500} + \sum_{j=1}^{25}\frac{1}{j + \sum_{i=1}^{2}(x_i - a_{ij})^6}\right)^{-1}$	2	[−65, 65]	1
$F_{15}(x) = \sum_{i=1}^{11}\left[a_i - \frac{x_1(b_i^2 + b_i x_2)}{b_i^2 + b_i x_3 + x_4}\right]^2$	4	[−5, 5]	0.00030
$F_{16}(x) = 4x_1^2 - 2.1x_1^4 + \frac{1}{3}x_1^6 + x_1x_2 - 4x_2^2 + 4x_2^4$	2	[−5, 5]	−1.0316
$F_{17}(x) = \left(x_2 - \frac{5.1}{4\pi^2}x_1^2 + \frac{5}{\pi}x_1 - 6\right)^2 + 10\left(1 - \frac{1}{8\pi}\right)\cos x_1 + 10$	2	[−5, 5]	0.398
$F_{18}(x) = \left[1 + (x_1 + x_2 + 1)^2\left(19 - 14x_1 + 3x_1^2 - 14x_2 + 6x_1x_2 + 3x_2^2\right)\right] \times \left[30 + (2x_1 - 3x_2)^2\left(18 - 32x_1 + 12x_1^2 + 48x_2 - 36x_1x_2 + 27x_2^2\right)\right]$	2	[−2, 2]	3
$F_{19}(x) = -\sum_{i=1}^{4} c_i \exp\left(-\sum_{j=1}^{3} a_{ij}\left(x_j - p_{ij}\right)^2\right)$	3	[1, 3]	−3.86
$F_{20}(x) = -\sum_{i=1}^{4} c_i \exp\left(-\sum_{j=1}^{6} a_{ij}\left(x_j - p_{ij}\right)^2\right)$	6	[0, 1]	−3.32
$F_{21}(x) = -\sum_{i=1}^{5}\left[(X - a_i)(X - a_i)^T + c_i\right]^{-1}$	4	[0, 10]	−10.1562
$F_{22}(x) = -\sum_{i=1}^{7}\left[(X - a_i)(X - a_i)^T + c_i\right]^{-1}$	4	[0, 10]	−10.4028
$F_{23}(x) = -\sum_{i=1}^{10}\left[(X - a_i)(X - a_i)^T + c_i\right]^{-1}$	4	[0, 10]	−10.5363

Table 24 Detailed description of composite benchmark functions

Functions	Dimension	Range	f_{min}
CF1	30	[−5, 5]	0
$f_1, f_2, f_3, ..., f_{10} = F_1$			
$[\sigma_1, \sigma_2, \sigma_3, ..., \sigma_{10}] = [1, 1, 1, ..., 1]$			
$[\lambda_1, \lambda_2, \lambda_3, ..., \lambda_{10}] = [5/100, 5/100, 5/100, ..., 5/100]$			
CF2	30	[−5, 5]	0
$f_1, f_2, f_3, ..., f_{10} = F_1$			
$[\sigma_1, \sigma_2, \sigma_3, ..., \sigma_{10}] = [1, 1, 1, ..., 1]$			
$[\lambda_1, \lambda_2, \lambda_3, ..., \lambda_{10}] = [5/100, 5/100, 5/100, ..., 5/100]$			
CF3	30	[−5, 5]	0
$f_1, f_2, f_3, ..., f_{10} = F_1$			
$[\sigma_1, \sigma_2, \sigma_3, ..., \sigma_{10}] = [1, 1, 1, ..., 1]$			
$[\lambda_1, \lambda_2, \lambda_3, ..., \lambda_{10}] = [1, 1, 1, ..., 1]$			
CF4	30	[−5, 5]	0
$f_1, f_2 = F_{10}$			
$f_3, f_4 = F$			
$f_5, f_6 =$ Weierstrass function			
$f_7, f_8 = F_{11}$			
$f_9, f_{10} = F_1$			
$[\sigma_1, \sigma_2, \sigma_3, ..., \sigma_{10}] = [1, 1, 1, ..., 1]$			
$[\lambda_1, \lambda_2, \lambda_3, ..., \lambda_{10}] = [5/32, 5/32, 1, 1, 5/0.5, 5/0.5, 5/100, 5/100, 5/100, 5/100]$			
CF5	30	[−5, 5]	0
$f_1, f_2 = F_9$			
$f_3, f_4 =$ Weierstrass function			
$f_5, f_6 = F_{11}$			
$f_7, f_8 = F_{10}$			
$f_9, f_{10} = F_1$			
$[\sigma_1, \sigma_2, \sigma_3, ..., \sigma_{10}] = [1, 1, 1, ..., 1]$			
$[\lambda_1, \lambda_2, \lambda_3, ..., \lambda_{10}] = [1/5, 1/5, 5/0.5, 5/0.5, 5/100, 5/100, 5/32, 5/32, 5/100, 5/100]$			
CF6	30	[−5, 5]	0
$f_1, f_2 = F_9$			
$f_3, f_4 =$ Weierstrass function			
$f_5, f_6 = F_{11}$			
$f_7, f_8 = F_{10}$			
$f_9, f_{10} = F_1$			
$[\sigma_1, \sigma_2, \sigma_3, ..., \sigma_{10}] = [0.1, 0.2, 0.3, 0.4, 0.5, 0.6, 0.7, 0.8, 0.9, 1]$			
$[\lambda_1, \lambda_2, \lambda_3, ..., \lambda_{10}] = [0.1 * 1/5, 0.2 * 1/5, 0.3 * 5/0.5, 0.4 * 5/0.5, 0.5 * 5/100,$ $0.6 * 5/100, 0.7 * 5/32, 0.8 * 5/32, 0.9 * 5/100, 1 * 5/100]$			
$\text{Weierstrass} = \sum_{i=1}^{n}\left(\sum_{k=0}^{k\max}\left[a^k \cos\left(2\pi b^k (x_i + 0.5)\right)\right]\right) - n\sum_{k=0}^{k\max}\left[a^k \cos\left(2\pi b^k 0.5\right)\right],\ a = 0.5,\ b = 3,\ k\max = 20$			

Table 25 Power generation limit, cost and emission coefficient for thermal units

Units	Power limit (MW)		Cost coefficients					Emission coefficients				
	$P_{Th,min}$	$P_{Th,max}$	α_{Th}	β_{Th}	γ_{Th}	δ_{Th}	ϵ_{Th}	b_0	b_1	b_2	b_3	b_4
1	20	175	0.0012	2.45	100	160	0.038	60	− 1.355	0.0105	0.4968	0.01925
2	40	300	0.001	2.32	120	180	0.037	45	− 0.6	0.008	0.486	0.01694
3	50	500	0.0015	2.1	150	200	0.035	30	− 0.555	0.012	0.5035	0.01478

Table 26 Transport delay of reservoir units

Plant Number	Plant 1	Plant 2	Plant 3	Plant 4
RU	0	0	2	1
Time (h)	2	3	4	0

Table 27 Reservoir inflows of hydro units for 24 h

Hour	Inflow water (m^3)				Hour	Inflow water (m^3)			
	I_1	I_2	I_3	I_4		I_1	I_2	I_3	I_4
1	100,000	80,000	81,000	28,000	13	110,000	80,000	40,000	0
2	90,000	80,000	82,000	24,000	14	120,000	90,000	30,000	0
3	80,000	90,000	40,000	16,000	15	110,000	90,000	30000	0
4	70,000	90,000	20,000	0	16	100,000	80,000	20,000	0
5	60,000	80,000	30,000	0	17	90,000	70,000	20,000	0
6	70,000	70,000	40,000	0	18	80,000	60,000	20,000	0
7	80,000	60,000	30,000	0	19	70,000	70,000	10,000	0
8	90,000	70,000	20,000	0	20	60,000	80,000	10,000	0
9	100,000	80,000	10,000	0	21	70,000	90,000	20,000	0
10	110,000	90,000	10,000	0	22	80,000	90,000	20,000	0
11	120,000	90,000	10,000	0	23	90,000	80,000	10,000	0
12	100,000	80,000	20,000	0	24	100,000	80,000	0	0

Table 28 Reservoir capacity, reservoir initial and end conditions, discharge and generation limit

Plant	$v_{H,min}$ (m^3)	$v_{H,max}$ (m^3)	v_H^{ini} (m^3)	v_H^{fin} (m^3)	$q_{H,min}$ (m^3)	$q_{H,max}$ (m^3)	$P_{H,min}$ (MW)	$P_{H,max}$ (MW)
1	800,000	1,500,000	1,000,000	1,200,000	50,000	150,000	0	500
2	600,000	1,200,000	800,000	700,000	60,000	150,000	0	500
3	1,000,000	2,400,000	1,700,000	1,700,000	100,000	300,000	0	500
4	700,000	1,600,000	1,200,000	1,400,000	60,000	200,100	0	500

Table 29 Coefficient of hydro units

Plant	c_1	c_2	c_3	c_4	c_5	c_6
1	− 0.0042	− 0.42	0.03	0.9	10	-50
2	− 0.004	− 0.3	0.015	1.14	9.5	-70
3	− 0.0016	− 0.3	0.014	0.55	5.5	-40
4	− 0.003	− 0.31	0.027	1.44	14	-90

Table 30 Transmission loss coefficient (*B*-coefficient) of 7-unit system

B Transmission loss coefficients

$$10\text{-}7\ X \begin{bmatrix} 49 & 14 & 15 & 15 & 20 & 17 & 17 \\ 14 & 45 & 16 & 20 & 18 & 15 & 15 \\ 15 & 16 & 39 & 10 & 12 & 12 & 14 \\ 15 & 20 & 10 & 40 & 14 & 10 & 11 \\ 20 & 18 & 12 & 14 & 35 & 11 & 13 \\ 17 & 15 & 12 & 10 & 11 & 36 & 12 \\ 17 & 15 & 14 & 11 & 13 & 12 & 38 \end{bmatrix}$$

Table 31 Number of turbines, velocity and coefficient of wind generating units

Units	Turbine	W_r	l	c	v_{in} (m/s)	v_{out} (m/s)	v_r (m/s)	C_0	C_u
1st	30	3	1.8862	4.6024	4	25	16	30	5
2nd	20	3	1.7128	4.4363	3	25	13	20	5

Table 32 24 h load demand, temperature and solar radiation

Hour	P_D (MW)	T	R (Watt/m^2)	Hour	P_D (MW)	T	R (Watt/m^2)
1	750	30	0	13	1110	37	1013.5
2	780	29	0	14	1030	37	848.2
3	700	28	0	15	1010	37	726.7
4	650	28	0	16	1060	38	654
5	670	28	5.4	17	1050	38	392.9
6	800	28	101	18	1120	37	215.1
7	950	29	253.7	19	1070	35	38.5
8	1010	31	541.2	20	1050	34	0
9	1090	33	530.4	21	910	34	0
10	1080	34	739.9	22	860	33	0
11	1100	35	1078	23	850	32	0
12	1150	36	1125.6	24	800	32	0

Table 33 Generation of solar power and unit rate of solar units

Solar panel	P_S (MW)	Unit rate ($/MW)
1	20	0.22
2	25	0.23
3	25	0.23
4	30	0.24
5	30	0.24
6	35	0.25
7	35	0.26
8	40	0.27
9	40	0.27
10	40	0.275
11	40	0.28
12	40	0.28
13	40	0.28

Table 34 Power generation limit and ramp rate limits for thermal units of Test system-2

Units	Power limit (MW)		Ramp rate limit	
	$P_{Th,\min}$	$P_{Th,\max}$	ur	dr
1	20	350	85	85
2	40	300	100	85
3	50	500	90	90

Table 35 Transmission loss coefficient (B-coefficient) of 11-unit system

B Transmission loss coefficients											
	[49	14	15	15	16	17	17	18	19	20	19
	14	45	16	16	17	15	15	16	18	18	18
	15	16	39	10	12	12	14	14	16	16	16
	15	16	10	40	14	10	11	12	14	15	14
	16	17	12	14	35	11	13	13	15	16	15
10-7 X	17	15	12	10	11	36	12	12	14	15	14
	17	15	14	11	13	12	38	16	16	18	16
	18	16	14	12	13	12	16	40	15	16	15
	19	18	16	14	15	14	16	15	42	19	42
	20	18	16	15	16	15	18	16	19	44	19
	19	18	16	14	15	14	16	15	42	19	46]

References

Abido M (2009) Multiobjective particle swarm optimization for environmental/economic dispatch problem. Electr Power Syst Res 79(7):1105–1113

Acharya S, Ganesan S, Kumar DV, Subramanian S (2021) A multi-objective multi-verse optimization algorithm for dynamic load dispatch problems. Knowl Based Syst 107411

Aljarah I, Faris H, Heidari AA et al (2021) A robust multi-objective feature selection model based on local neighborhood multi-verse optimization. IEEE Access 9:100009–100028

Basu Mousumi (2006) Bi-objective generation scheduling of fixed head hydrothermal power systems through an interactive fuzzy satisfying method and particle swarm optimization. Int J Emerg Electr Power Syst 6(1)

Basu M (2004) An interactive fuzzy satisfying method based on evolutionary programming technique for multiobjective short-term hydrothermal scheduling. Electr Power Syst Res 69(2–3):277–285

Basu M (2019) Multi-area dynamic economic emission dispatch of hydro-wind-thermal power system. Renew Energy Focus 28:11–35

Bhattacharjee K, Bhattacharya A, Dey NSH (2014) Real coded chemical reaction based optimization for short-term hydrothermal scheduling. Appl Soft Comput 24:962–976

Borghetti A, D'Ambrosio C, Lodi A, Martello S (2008) An MILP approach for short-term hydro scheduling and unit commitment with head-dependent reservoir. IEEE Trans Power Syst 23(3):1115–1124

Cavazzini G, Pavesi G, Ardizzon G (2018) A novel two-swarm based PSO search strategy for optimal short-term hydro-thermal generation scheduling. Energy Convers Manag 164:460–481

Chen F, Zhou J, Wang C, Li C, Lu P (2017) A modified gravitational search algorithm based on a non-dominated sorting genetic approach for hydro-thermal-wind economic emission dispatching. Energy 121:276–291

Dasgupta K, Roy PK, Mukherjee V (2020) Power flow based hydro-thermal-wind scheduling of hybrid power system using sine cosine algorithm. Electr Power Syst Res 178:106018

Dasgupta K, Roy PK, Mukherjee V (2022) Solution of short term integrated hydrothermal-solar-wind scheduling using sine cosine algorithm. Energy Strat Rev 40:100824

Dey SK, Dash DP, Basu M (2022) Application of NSGA-II for environmental constraint economic dispatch of thermal-wind-solar power system. Renew Energy Focus 43:239–245

Dhiman G (2020) MOSHEPO: a hybrid multi-objective approach to solve economic load dispatch and micro grid problems. Appl Intell 50(1):119–137

Genc A, Erisoglu M, Pekgor A, Oturanc G, Hepbasli A, Ulgen K (2005) Estimation of wind power potential using Weibull distribution. Energy Sources 27(9):809–822

Gouthamkumar N, Sharma V, Naresh R (2015) Disruption based gravitational search algorithm for short term hydrothermal scheduling. Expert Syst Appl 42(20):7000–7011

Gul E, Kang C, Wang J (2019) Multi-objective short-term integration of hydrothermal operation with wind and solar power using nonlinear programming. Energy Procedia 158:6274–6281

Hazra S, Roy PK (2020) Optimal dispatch using moth-flame optimization for hydro-thermal-wind scheduling problem. Int Trans Electr Energy Syst 30(8):e12460

Hazra S, Roy P (2021) Solar-wind-hydro-thermal scheduling using moth flame optimization. Optim Control Appl Methods **(First published on 09 September 2021)**

Hota P, Barisal A, Chakrabarti R (2009) An improved PSO technique for short-term optimal hydrothermal scheduling. Electr Power Syst Res 79(7):1047–1053

Ji B, Zhang B, Samson SY, Zhang D, Yuan X (2021) An enhanced Borg algorithmic framework for solving the hydro-thermal-wind Co-scheduling problem. Energy 218:119512

Jin-Shyr Y, Nanming C (1989) Short term hydrothermal coordination using multi-pass dynamic programming. IEEE Trans Power Syst 4(3):1050–1056

Li X, Du D, Pei J, Menhas M (2013) Probabilistic load flow calculation with Latin hypercube sampling applied to grid-connected induction wind power system. Trans Inst Meas Control 35(1):56–65

Li W, Meng X, Huang Y, Mahmoodi S (2021) Knowledge-guided multiobjective particle swarm optimization with fusion learning strategies. Complex Intell Syst 7(3):1223–1239

Liu Z, Zhang Z, Zhuo R, Wang X (2019) Optimal operation of independent regional power grid with multiple wind-solar-hydro-battery power. Appl Energy 235:1541–1550

Mandal KK, Chakraborty N (2009) Short-term combined economic emission scheduling of hydrothermal power systems with cascaded reservoirs using differential evolution. Energy Convers Manag 50(1):97–104

Mirjalili S, Lewis A (2016) The whale optimization algorithm. Adv Eng Softw 95:51–67

Mirjalili S, Jangir P, Mirjalili SZ, Saremi S, Trivedi IN (2017) Optimization of problems with multiple objectives using the multi-verse optimization algorithm. Knowl Based Syst 134:50–71

Mukherjee A, Mukherjee V (2015) Solution of optimal power flow using chaotic krill herd algorithm. Chaos Solitons Fractals 78:10–21

Narang N (2017) Short-term hydrothermal generation scheduling using improved predator influenced civilized swarm optimization technique. Appl Soft Comput 58:207–224

Nazari-Heris M, Mohammadi-Ivatloo B, Haghrah A (2017) Optimal short-term generation scheduling of hydrothermal systems by implementation of real-coded genetic algorithm based on improved Mühlenbein mutation. Energy 128:77–85

Nguyen TT, Vo DN, Truong AV (2014) Cuckoo search algorithm for short-term hydrothermal scheduling. Appl Energy 132:276–287

OuYang J, Yang F, Yang S, Nie Z (2008) The improved NSGA-II approach. J Electromagn Waves Appl 22(2–3):163–172

Panda A, Tripathy M, Barisal A, Prakash T (2017) A modified bacteria foraging based optimal power flow framework for Hydro-Thermal-Wind generation system in the presence of STATCOM. Energy 124:720–740

Parouha RP (2019) Nonconvex/nonsmooth economic load dispatch using modified time-varying particle swarm optimization. Comput Intell 35(4):717–744

Parouha RP, Verma P (2021) An innovative hybrid algorithm to solve nonconvex economic load dispatch problem with or without valve point effects. Int Trans Electr Energy Syst 31(1):e12682

Patwal RS, Narang N (2020) Optimal generation scheduling of pumped storage hydro-thermal system with wind energy sources. Appl Soft Comput 93:106345

Patwal RS, Narang N, Garg H (2018) A novel TVAC-PSO based mutation strategies algorithm for generation scheduling of pumped storage hydrothermal system incorporating solar units. Energy 142:822–837

Paul C, Roy PK, Mukherjee V (2020) Chaotic whale optimization algorithm for optimal solution of combined heat and power economic dispatch problem incorporating wind. Renew Energy Focus 35:56–71

Paul C, Roy PK, Mukherjee V (2021) Application of chaotic-quasi-oppositional whale optimization algorithm on CHPED problem integrated with wind-solar-EVs. Int Trans Electr Energy Syst **(Accepted on 09 September 2021)**

Paul C, Roy PK, Mukherjee V (2021) Study of wind-solar based combined heat and power economic dispatch problem using quasi-oppositional-based whale optimization technique. Optim Control Appl Methods **(Accepted on 02 September 2021)**

Petcharaks N, Ongsakul W (2007) Hybrid enhanced Lagrangian relaxation and quadratic programming for hydrothermal scheduling. Electr Power Comp Syst 35(1):19–42

Qing X, Niande X, Shiying W, Boming Z, Mei H (1988) Optimal daily scheduling of cascaded plants using a new algorithm of nonlinear minimum cost network flow. IEEE Trans Power Syst 3(3):929–935

Rahnamayan S, Tizhoosh HR, Salama MM (2008) Opposition versus randomness in soft computing techniques. Appl Soft Comput 8(2):906–918

Roy PK (2013) Teaching learning based optimization for short-term hydrothermal scheduling problem considering valve point effect and prohibited discharge constraint. Int J Electr Power Energy Syst 53:10–19

Roy PK, Pradhan M, Paul T (2018) Krill herd algorithm applied to short-term hydrothermal scheduling problem. Ain Shams Eng J 9(1):31–43

Salam MS, Nor KM, Hamdam A (1998) Hydrothermal scheduling based Lagrangian relaxation approach to hydrothermal coordination. IEEE Trans Power Syst 13(1):226–235

Shu S, Mo L, Wang Y (2019) Peak saving strategy of wind-solar-hydro hybrid generation system based on modified differential evolution algorithm. Energy Procedia 158:3500–3505

Šulek P, Orfánus M, Dušička P (2014) Optimizing hydro power reservoir system using hybrid optimization approach 511–518

Sundaram A (2022) Multiobjective multi verse optimization algorithm to solve dynamic economic emission dispatch problem with transmission loss prediction by an artificial neural network. Appl Soft Comput 109021

Sundaram Arunachalam (2017) Solution of combined economic emission dispatch problem with valve-point effect using hybrid NSGA II-MOPSO. Part Swarm Optim Appl

Sundaram A (2020) Multiobjective multi-verse optimization algorithm to solve combined economic, heat and power emission dispatch problems. Appl Soft Comput 91:106195

Wang M, Lu G (2021) A modified sine cosine algorithm for solving optimization problems. IEEE Access 9:27434–27450

Wang Y, Zhou J, Mo L, Zhang R, Zhang Y (2012) Short-term hydrothermal generation scheduling using differential real-coded quantum-inspired evolutionary algorithm. Energy 44(1):657–671

Wang X, Chang J, Meng X, Wang Y (2018) Short-term hydro-thermal-wind-photovoltaic complementary operation of interconnected power systems. Appl Energy 229:945–962

Wang WL, Li WK, Wang Z, Li L (2019) Opposition-based multi-objective whale optimization algorithm with global grid ranking. Neurocomputing 341:41–59

Wei H, Hongxuan Z, Yu D, Yiting W, Ling D, Ming X (2019) Short-term optimal operation of hydro-wind-solar hybrid system with improved generative adversarial networks. Appl Energy 250:389–403

Yin X, Cheng L, Wang X, Lu J, Qin H (2019) Optimization for hydro-photovoltaic-wind power generation system based on modified version of multi-objective whale optimization algorithm. Energy Procedia 158:6208–6216

Zhang J, Wang J, Yue C (2011) Small population-based particle swarm optimization for short-term hydrothermal scheduling. IEEE Trans Power Syst 27(1):142–152

Zhang L, Mistry K, Neoh SC, Lim CP (2016) Intelligent facial emotion recognition using moth-firefly optimization. Knowl Based Syst 111:248–267

Zhao S, Fang Y, Wei Z (2019) Stochastic optimal dispatch of integrating concentrating solar power plants with wind farms. Int J Electr Power Energy Syst 109:575–583

Zou D, Li S, Kong X, Ouyang H, Li Z (2019) Solving the combined heat and power economic dispatch problems by an improved genetic algorithm and a new constraint handling strategy. Appl Energy 237:646–670